ments [ELISA assay (direct or extraction method) or RIA], and (*c*) consistently good overall general condition. Any subjects with abnormal physical findings were excluded. The control infants were without neurologic and endocrinologic abnormalities, and none of the subjects received antenatal or perinatal glucocorticoid before urine sampling. Table 1 shows characteristics of the study subjects.

Spot urine samples were randomly collected for the study and kept at −20 °C until analysis. We studied each infant for urinary steroid profile by GC-MS/selected ion monitoring (GC-MS-SIM), as reported *(8)* with minor modification. In brief, 0.05- to 0.2-mL urine samples were subjected enzymatic hydrolysis and organic solvent extraction and methyloxime-trimethylsilyl derivatized, and the derivative was subjected to GC-MS-SIM analysis. GC-MS-SIM analysis was performed on an HP5890II GC with an HP-Ultra1 fused silica column (25 m × 0.2 nm × 0.33 μm) coupled to an HP5971MS (Agilent Technologies). We quantified each steroid with stigmasterol as the internal standard. The turnaround time of the assay is 2 days.

We measured Ptl and the cortisol metabolites 5α-tetrahydrocortisone and 5β-tetrahydrocortisone (sum of these metabolites termed THEs) and calculated the ratio of Ptl to the cortisol metabolites (Ptl/THEs) *(5, 9)* to differentiate C21OHD and PORD from TH17OHP and controls. Ptl was considered to be equal to 0.001 mg/g creatinine for calculation in infants whose Ptl was under the detection limit (<0.001 mg/g creatinine). We measured metabolites of 3 steroids, namely dehydroepiandrosterone (DHEA), androstenedione (AD4), and 11β-hydroxyandrostenedione (11OHAD4), and calculated the sum of DHEA metabolites (DHEA, androstenediol, 16α-hydroxy-DHEA, 16β-hydroxy-DHEA, 16-oxo-androstenediol, and androstenetriol), the sum of AD4 metabolites (androsterone and etiocholanolone) *(8, 10)*, and the 11OHAD4 metabolite (11HA). (11β-Hydroxyetiocholanolone could not be measured in newborns, as described *(8)*.) The above sum of DHEA metabolites have been reported to include approximately 70% of DHEA metabolites in newborns *(11)*. The above sum of AD4 metabolites are defined as androgen metabolites because, whereas these 2 steroids are metabolites of AD4, they are also the metabolites of testosterone and dihydrotestosterone in boys. Androgen metabolites are analyzed separately by sex, since male androgen metabolites in this age group are increased from testicular-derived androsterone and etiocholanolone.

We measured urinary creatinine by IATRO-LQ CRE (A)II (Mitsubishi Chemical Medience Co.) and expressed urinary steroid concentration relative to urinary creatinine (mg/g creatinine).

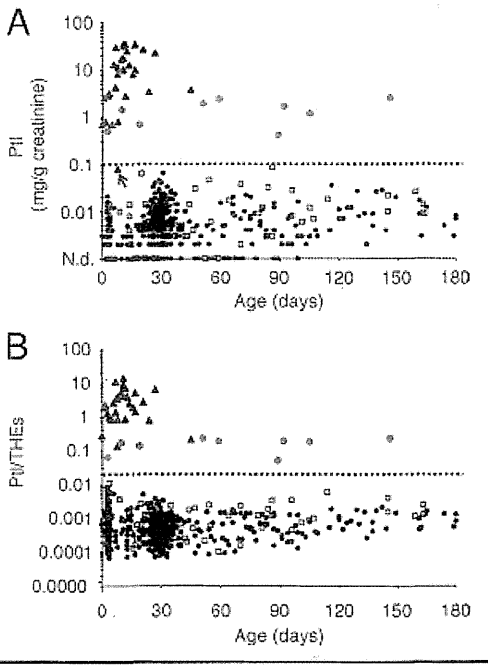

Fig. 2. Urinary (A) Ptl and Ptl/THEs (B) in infants with C21OHD, PORD, TH17OHP, and controls.

Dashed lines show cutoff: Ptl, 0.1 mg/g creatinine; Ptl/THEs, 0.020. ▲, C21OHD; ●, PORD; □, TH17OHP; ●, control. An arrow points to the patient with C21OHD at a lower Ptl value than the cutoff. N.d., not detected.

Statistical analysis of DHEA, androgen, and 11OHAD4 metabolites was carried out by Mann–Whitney *U*-test between C21OHD and PORD. A *P* value of <0.05 was considered statistically significant.

Results

DIFFERENTIATION OF C21OHD AND PORD FROM TH17OHP AND CONTROLS

Fig. 2 shows the results of urinary Ptl and Ptl/THEs. Ptl [median (range) mg/g creatinine] was 10 (0.079–36) in C21OHD, 1.5 (0.42–2.6) in PORD, 0.006 (<0.001–0.086) in TH17OHP, and <0.001 (<0.001–0.064) in controls. Ptl/THEs was 2.5 (0.14–15) in C21OHD, 0.18 (0.051–0.23) in PORD, 0.00083 (0.00010–0.011) in TH17OHP, and 0.00038 (0.000068–0.0083) in controls. Ptl differentiated C21OHD and PORD from TH17OHP and controls with 96.9% (95% CI 91.6%–97.4%) sensitivity and 100% (99.8%–100%) specificity with cutoff 0.1 mg/g creatinine. All patients with TH17OHP and controls showed Ptl concentrations below the cutoff. An 8-day-old patient with C21OHD whose birth weight was 1628 g had a lower Ptl value

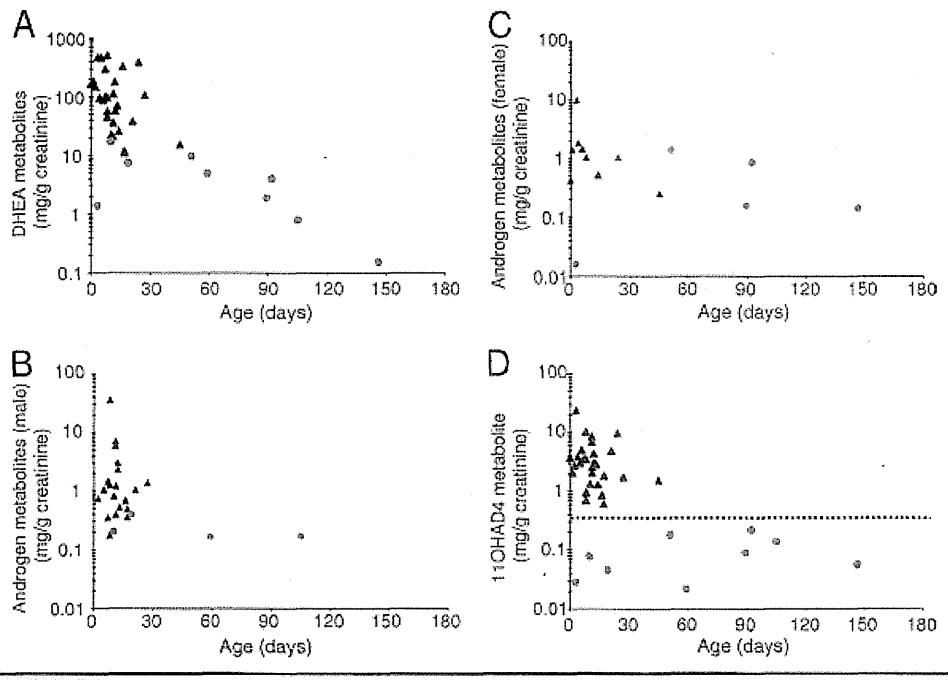

Fig. 3. Urinary metabolites of 17,20-lyase products DHEA (A), androgen (male) (B), androgen (female) (C), and 11OHAD4 (D) in infants with C21OHD and PORD.

Dashed line in (D) shows cutoff of 0.35 mg/g creatinine for 11OHAD4 metabolite. ▲, C21OHD; ●, PORD.

than the cutoff (Fig. 2A, arrow). Ptl/THEs differentiated C21OHD and PORD from TH17OHP and control with 100% (95.1%–100%) diagnostic sensitivity and 100% (99.8%–100%) diagnostic specificity with the 0.020 cutoff.

DISCRIMINATION BETWEEN C21OHD AND PORD

Fig. 3 shows the results of urinary metabolites of 17,20-lyase products (mg/g creatinine) in C21OHD and PORD. DHEA metabolites were 97 (11–505) in C21OHD and 4.0 (0.15–17) in PORD. Androgen metabolites were, for boys, 1.1 (0.18–36) in C21OHD and 0.19 (0.17–0.41) in PORD, and for girls, 1.1 (0.26–9.9) in C21OHD and 0.16 (0.016–1.4) in PORD. 11OHAD4 metabolite was 3.0 (0.61–24) in C21OHD and 0.077 (0.022–0.22) in PORD. All metabolites of 17,20-lyase products showed significant differences between C21OHD and PORD (DHEA metabolites, $P < 0.001$; androgen metabolites (male), $P = 0.006$; androgen metabolites (female), $P = 0.039$; 11OHAD4 metabolite, $P < 0.001$). 11OHAD4 metabolite (11HA) discriminated between C21OHD and PORD with 100% (94.2%–100%) diagnostic sensitivity and 100% (81.4%–100%) diagnostic specificity with the 0.35 mg/g creatinine cutoff. Urinary DHEA and androgen metabolites showed overlap between C21OHD and PORD.

Discussion

We established a 2-step biochemical differential diagnosis for C21OHD and PORD by urinary steroid profile. First, by using a specific cutoff of the ratio of Ptl to THEs, we were able to differentiate C21OHD and PORD from TH17OHP and controls. Second, by using a specific cutoff of 11HA, we were able to distinguish between C21OHD and PORD. Although a distinctive steroid excretion pattern in C21OHD and PORD had been reported *(3, 5, 6)*, no clear cutoff of urinary steroid metabolites was reported in any ages to discriminate between C21OHD and PORD. To the best of our knowledge, this is the first report of a cutoff for biochemical differential diagnosis of C21OHD and PORD in infants. As for TH17OHP, an adequate observation period and timing for repeat blood test are as yet unknown. It is difficult to differentiate between C21OHD and PORD by current standard hormonal testing and clinical observation *(3, 4)*. This 2-step method can diagnose TH17OHP, C21OHD, and PORD by 1 as-

say with a noninvasive spot urine sample while infants have increased concentrations of serum 17OHP.

Increased Ptl and Ptl/THEs in C21OHD and PORD must reflect the impaired activity of 21-hydroxylase. We showed that a specific cutoff of Ptl/THEs differentiated C21OHD and PORD from TH17OHP and controls with no overlap. In patients with C21OHD, impaired activity of 21-hydroxylase led to an increase in the precursor steroid 17OHP. As a result, Ptl, which is a metabolite of 21DOF, was increased. Because the activity of 21-hydroxylase in patients with PORD was impaired by less electron supply from POR, increased Ptl was reasonable.

Decreased 11HA in PORD must reflect the impaired activity of 17,20-lyase. The reason is unclear why the urinary 11OHAD4 metabolite was the only 1 among other metabolites of 17,20-lyase products that showed a difference between C21OHD and PORD, but the reason is probably that 11OHAD4 is of purely adrenal origin. DHEA metabolites showed tiny overlap between C21OHD and PORD that may derive from unexpectedly low DHEA metabolites in 3 patients with C21OHD. On the 1 hand, androgen metabolites showed a clear overlap that can be explained by androgen production in the backdoor pathway (Fig. 1, dashed arrow), which is proven in the tammar wallaby *(12)* and postulated in the human newborn *(13)*. Androsterone can be derived not only from AD4 and dihydrotestosterone in the conventional pathway but also from 5α-pregnane-3α,17α-diol-20-one in the backdoor pathway *(12, 13)*. In PORD, androsterone could increase during early infancy *(13)*, resulting in overlap in androgen metabolites.

One may argue that PD, the ratio of PD to 17,20-lyase metabolites (e.g., 11HA, DHEA metabolites), or the ratio of 17α-hydroxypregnenolone metabolite to DHEA metabolites *(13)* is discriminatory (Fig. 1). Unfortunately, the measurement of PD is sometimes problematic in our GC-MS method in newborns and we cannot calculate the concentration or the ratio. We have reported that the ratio of 17α-hydroxypregnenolone metabolites to DHEA metabolites discriminated 22 patients with PORD from healthy infants *(13)*, whereas this ratio could not discriminate C21OHD and PORD completely in this cohort (data not shown).

This study had 4 limitations. First, nonclassic 21OHD was not included in study subjects. Nonclassic 21OHD is known to have lower blood 17OHP than C21OHD *(14, 15)*. Thus, it is conceivable that these individuals have lower Ptl/THEs and 11HA than C21OHD. Further studies are required to determine if the same cutoff can discriminate between nonclassic 21OHD and PORD. Second, the total number of affected infants, and specifically the number of very-low-birthweight infants (only 2), was limited in this study. Infants born with very low birthweight should have less hepatic enzyme activities such as 5β-reductase, 3α-hydroxysteroid dehydrogenase, and 20α-hydroxysteroid dehydrogenase, leading to less conversion of 21DOF to Ptl. Indeed, 1 patient with C21OHD who was born with low birthweight had a lower Ptl value than the cutoff. The third limitation is the random time at which urine samples were collected, although it is known that steroid metabolism starts to show diurnal variation around 2–3 months of age *(16)*. We unintentionally proved that we could use the urine sample whenever it is collected. As for the fourth limitation, our data in Japanese infants may not apply to other ethnic populations. Enzymatic residual activity in PORD has been reported to differ depending on genotype *(17)*. The common mutation was R457H in Japanese PORD *(7, 18)* and A287P in whites *(19)*. R457H has 1%–3% supporting activity for 17α-hydroxylase and virtually no activity for 17,20-lyase compared to wild type, whereas A287P has 40% activity for 17α-hydroxylase and about 20% for 17,20-lyase *(17, 19, 20)*. In fact, all subjects with PORD were Japanese with homozygous or heterozygous R457H mutation (Table 2). For PORD cohorts with higher 17,20-lyase activity (i.e., A287P), 11HA might not be as useful. Thus other cutoffs may be required for non-Japanese.

In conclusion, we demonstrated a 2-step biochemical differential diagnosis for C21OHD and PORD by urinary steroid metabolites such as Ptl, THEs, and 11HA. We believe that this 2-step biochemical diagnosis would be valuable for Japanese infants whose clinical differential diagnosis is difficult.

Author Contributions: *All authors confirmed they have contributed to the intellectual content of this paper and have met the following 3 requirements: (a) significant contributions to the conception and design, acquisition of data, or analysis and interpretation of data; (b) drafting or revising the article for intellectual content; and (c) final approval of the published article.*

Authors' Disclosures or Potential Conflicts of Interest: *Upon manuscript submission, all authors completed the Disclosures of Potential Conflict of Interest form. Potential conflicts of interest:*

Employment or Leadership: None declared.
Consultant or Advisory Role: None declared.
Stock Ownership: None declared.
Honoraria: None declared.
Research Funding: Funded by Health and Labor Sciences Research Grants for the Research on Intractable Disease from Ministry of Health, Labor, and Welfare in Japan; Grants-in-Aid for Scientific Research from the Japan Society for the Promotion of Science; and a Grant-in-Aid for Scientific Research on Innovative Areas from the Ministry of Education, Culture, Sports, Science, and Technology.
Expert Testimony: None declared.

Role of Sponsor: The funding organizations played no role in the design of study, choice of enrolled patients, review and interpretation of data, or preparation or approval of manuscript.

Acknowledgments: We thank Dr. Makoto Anzo, Dr. Katsumi Goji, Dr. Keiichi Hara, Dr. Kazunori Sanayama, Dr. Kazuhiro Mori, Dr. Keisuke Nagasaki, Dr. Shinji Nomura, Dr. Makoto Ono, Dr. Nobutaka Sasaki, Dr. Kimihira Seki, Dr. Eri Suzuki, Dr. Ikuko Takahashi, Dr. Noriyuki Takubo, Dr. Shiho Tamaura, and Dr. Etsushi Tsuchida for giving us valuable case samples. We also thank Dr. Misa Honda for critical comments and language editing.

References

1. Nimkarn S, Lin-Su K, New MI. Steroid 21 hydroxylase deficiency congenital adrenal hyperplasia. Endocrinol Metab Clin North Am 2009;38: 699–718.
2. Miller WL. P450 oxidoreductase deficiency: a new disorder of steroidogenesis with multiple clinical manifestations. Trends Endocrinol Metab 2004; 15:311–5.
3. Fukami M, Hasegawa T, Horikawa R, Ohashi T, Nishimura G, Homma K, Ogata T. Cytochrome P450 oxidoreductase deficiency in three patients initially regarded as having 21-hydroxylase deficiency and/or aromatase deficiency: diagnostic value of urine steroid hormone analysis. Pediatr Res 2006;59:276–80.
4. Stewart PM. The adrenal cortex. In: Larsen PR, Kronenberg HM, Melmed S, Polonsky KS (eds) Williams textbook of endocrinology, 10th ed. Philadelphia: Saunders 2002;491–551.
5. Homma K, Hasegawa T, Takeshita E, Watanabe K, Anzo M, Toyoura T, et al. Elevated urine pregnanetriolone definitively establishes the diagnosis of classical 21-hydroxylase deficiency in term and preterm neonates. J Clin Endocrinol Metab 2004;89:6087–91.
6. Shackleton C, Marcos J, Malunowicz EM, Szarras-Czapnik M, Jira P, Taylor NF, et al. Biochemical diagnosis of Antley-Bixler syndrome by steroid analysis. Am J Med Genet A 2004;128:A223–31.
7. Fukami M, Nishimura G, Homma K, Nagai T, Hanaki K, Uematsu A, et al. Cytochrome P450 oxidoreductase deficiency: identification and characterization of biallelic mutations and genotype-phenotype correlations in 35 Japanese patients. J Clin Endocrinol Metab 2009;94: 1723–31.
8. Homma K, Hasegawa T, Masumoto M, Takeshita E, Watanabe K, Chiba H, et al. Reference values for urinary steroids in Japanese newborn infants: gas chromatography/mass spectrometry in selected ion monitoring. Endocr J 2003;50:783–92.
9. Caulfield MP, Lynn T, Gottschalk ME, Jones KL, Taylor NF, Malunowicz EM, et al. The diagnosis of congenital adrenal hyperplasia in the newborn by gas chromatography/mass spectrometry analysis of random urine specimens. J Clin Endocrinol Metab 2002;87:3682–90.
10. Wudy SA, Hartmann MF. Gas chromatography-mass spectrometry profiling of steroids in times of molecular biology. Horm Metab Res 2004;36: 415–22.
11. Shackleton CH, Honour JW, Taylor NF. Metabolism of fetal and neonatal adrenal steroids. J Steroid Biochem 1979;11:523–9.
12. Wilson JD, Auchus RJ, Leihy MW, Guryev OL, Estabrook RW, Osborn SM, et al. 5alpha-Androstane-3alpha,17beta-diol is formed in tammar wallaby pouch young testes by a pathway involving 5alpha-pregnane-3alpha,17alpha-diol-20-one as a key intermediate. Endocrinology 2003;144:575–80.
13. Homma K, Hasegawa T, Nagai T, Adachi M, Horikawa R, Fujiwara I, et al. Urine steroid hormone profile analysis in cytochrome P450 oxidoreductase deficiency: implication for the backdoor pathway to dihydrotestosterone. J Clin Endocrinol Metab 2006;91:2643–9.
14. New MI. Extensive clinical experience: nonclassical 21-hydroxylase deficiency. J Clin Endocrinol Metab 2006;91:4205–14.
15. Kashimada K, Ono M, Onishi T, Koyama S, Toyoura T, Imai K, et al. Clinical course of patients with nonclassical 21-hydroxylase deficiency (21-OHD) diagnosed in infancy and childhood. Endocr J 2008;55:397–404.
16. Custodio RJ, Junior CE, Milani SL, Simões AL, de Castro M, Moreira AC. The emergence of the cortisol circadian rhythm in monozygotic and dizygotic twin infants: the twin-pair synchrony. Clin Endocrinol (Oxf) 2007;66:192–7.
17. Miller WL, Huang N, Agrawal V, Giacomini KM. Genetic variation in human P450 oxidoreductase. Mol Cell Endocrinol 2009;300:180–4.
18. Fukami M, Horikawa R, Nagai T, Tanaka T, Naiki Y, Sato N, et al. Cytochrome P450 oxidoreductase gene mutations and Antley-Bixler syndrome with abnormal genitalia and/or impaired steroidogenesis: molecular and clinical studies in 10 patients. J Clin Endocrinol Metab 2005;90: 414–26.
19. Huang N, Pandey AV, Agrawal V, Reardon W, Lapunzina PD, Mowat D, et al. Diversity and function of mutations in p450 oxidoreductase in patients with Antley-Bixler syndrome and disordered steroidogenesis. Am J Hum Genet 2005;76: 729–49.
20. Dhir V, Ivison HE, Krone N, Shackleton CH, Doherty AJ, Stewart PM, Arlt W. Differential inhibition of CYP17A1 and CYP21A2 activities by the P450 oxidoreductase mutant A287P. Mol Endocrinol 2007;21:1958–68.

Arch Gynecol Obstet (2012) 286:1079–1080
DOI 10.1007/s00404-012-2375-6

LETTER TO THE EDITOR

Deterioration of myocardial tissue Doppler indices in a case of fetal hydrothorax as a promising indication for clinical intervention before the development of nonimmune hydrops fetalis

Katsuyuki Sekii · Hiroaki Itoh · Tsutomu Ogata · Satoru Iwashima

Received: 11 March 2012 / Accepted: 7 May 2012 / Published online: 23 May 2012

Dear Editor,

The clinical course of fetal hydrothorax is highly variable between individuals, and its prenatal management varies from waiting and close observation to therapeutic intervention in utero or the termination of pregnancy. To date, the management of fetal hydrothorax has depended on the gestational age, rate of progression, and development of hydrops [1–3], partly because no appropriate indicator for clinical intervention is available before the onset of nonimmune hydrops fetalis (NIHF).

Tissue Doppler imaging (TDI) has been shown to be useful in assessing the cardiac function of fetuses with a normal [4] as well as pathological condition such as hydrops fetalis [5, 6]. So far, few studies have investigated the longitudinal cardiac function in fetal hydrothorax by TDI until hydropic change, and it has yet to be clarified whether serial TDI can provide clinical information concerning the indication for clinical intervention. We serially evaluated the fetal cardiac function with TDI in a case of fetal hydrothorax.

A 26-year-old primigravida woman was referred to our outpatient clinic for the evaluation of left unilateral fetal hydrothorax at 31 weeks and 6 days of gestation. An ultrasound scan digitally recorded at 25 weeks' gestation did not show hydrothorax. Serological examination showed no evidence of intrauterine infection, rhesus isoimmunization, or other red cell antibodies. Normal fetal anatomy and growth were confirmed by serial ultrasound scans. No other maternal or fetal complications were noted before admission. On admission at 32 weeks and 2 days of gestation, the unilateral lesion had proceeded to become bilateral. Betamethasone was administered maternally to promote fetal lung maturity. We conservatively managed the patient and closely evaluated fetal well-being and cardiac function in the fetus using fetal heart rate monitoring, the biophysical profile, umbilical artery Doppler velocimetry, and conventional pulsed-Doppler and tissue Doppler echocardiography to determine the appropriate timing of pregnancy termination for postnatal care, because of the institutional treatment strategy for fetal hydrothorax, whereby therapeutic intervention in utero, thoracocentesis, or pleuro-amniotic shunt, should be considered before 32 weeks of gestation.

During the first 3 days after admission, myocardial TDI parameters consistently increased with the gradual accumulation of pleural fluid and subcutaneous tissue thickening from 4 to 7 mm, although there were no apparent changes in conventional pulsed-Doppler parameters (Fig. 1), the biophysical profile, or fetal heart rate monitoring, and both ventricles were normal in size without mitral or tricuspid regurgitation.

The myocardial TDI parameters observed at 32 weeks and 4 days of gestation were even higher than the 95th percentile of the gestational age-based reference ranges for myocardial TDI indices [7]. We considered that the deterioration of the TDI parameters suggested the presence of subclinical or clinical cardiac dysfunction that could proceed to the development of NIHF, and so we decided to terminate the pregnancy. At 32 weeks and 4 days of gestation, a male infant weighing 1,920 g was delivered by

K. Sekii (✉) · T. Ogata · S. Iwashima
Department of Pediatrics, Hamamatsu University School of Medicine, 1-20-1 Handayama, Higashi-ku, Hamamatsu 431-3192, Japan
e-mail: sekii@hama-med.ac.jp

H. Itoh
Department of Obstetrics and Gynecology, Hamamatsu University School of Medicine, Hamamatsu, Japan

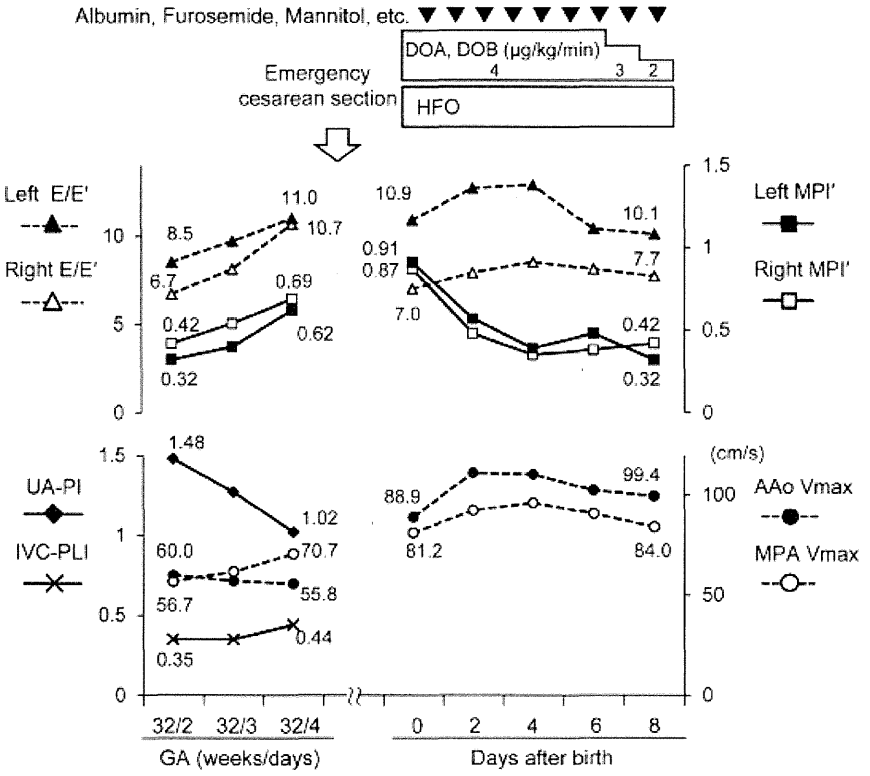

Fig. 1 Longitudinal changes in cardiac tissue Doppler and conventional pulsed-Doppler parameters before and after cesarean delivery followed by neonatal intensive care in the fetal and early neonatal heart. *DOA* dopamine, *DOB* dobutamine, *HFOV* high-frequency oscillatory ventilation, *E* peak early diastolic inflow velocity, *E'* myocardial peak velocity in early diastole, *MPI'* myocardial performance index measured by tissue Doppler imaging, *UA-PI* umbilical artery pulsatility index, *IVC-PLI* preload index of inferior vena cava, *AAo* ascending aorta, *MPA* main pulmonary artery, V_{max} maximum flow velocity, *GA* gestational age

emergency cesarean section, with Apgar scores of 6 and 8 at 1 and 5 min, respectively. The infant, with a structurally normal heart and moderate subcutaneous edema, became stable in response to intensive postnatal care, and myocardial TDI parameters gradually improved in the early neonatal period (Fig. 1). We considered that the timing of delivery for neonatal intervention had been appropriate, because intensive postnatal management successfully improved his cardiac function and clinical condition after birth.

The present case indicates that the deteriorated TDI parameters might be used as predictive indicators for the development of NIHF, and serial TDI may be a useful approach for making a decision regarding the timing of clinical intervention in pregnancies complicated by fetal hydrothorax. We suggest establishing a prospective cohort study with TDI evaluation, which may help us develop a new method of management for fetal hydrothorax.

Conflict of interest All authors declare that there is no actual or potential conflict of interest in relation to this letter. There were no external funding sources for this work.

References

1. Yinon Y, Kelly E, Ryan G (2008) Fetal pleural effusions. Best Pract Res Clin Obstet Gynaecol 22:77–96
2. Weber AM, Philipson EH (1992) Fetal pleural effusion: a review and meta-analysis for prognostic indicators. Obstet Gynecol 79:281–286
3. Abrams ME, Meredith KS, Kinnard P, Clark RH (2007) Hydrops fetalis: a retrospective review of cases reported to a large national database and identification of risk factors associated with death. Pediatrics 120:84–89
4. Sekii K, Ishikawa T, Ogata T, Itoh H, Iwashima S (2012) Fetal myocardial tissue Doppler indices before birth physiologically change in proportion to body size adjusted for gestational age in low-risk term pregnancies. Early Hum Dev. doi:10.1016/j.earlhumdev.2011.12.014
5. Aoki M, Harada K, Ogawa M, Tanaka T (2004) Quantitative assessment of right ventricular function using Doppler tissue imaging in fetuses with and without heart failure. J Am Soc Echocardiogr 17:28–35
6. Watanabe S, Hashimoto I, Saito K, Watanabe K, Hirono K, Uese K et al (2009) Characterization of ventricular myocardial performance in the fetus by tissue Doppler imaging. Circ J 73:943–947
7. Comas M, Crispi F, Gómez O, Puerto B, Figueras F, Gratacós E (2011) Gestational age- and estimated fetal weight-adjusted reference ranges for myocardial tissue Doppler indices at 24–41 weeks' gestation. Ultrasound Obstet Gynecol 37:57–64

OPEN ACCESS Freely available online PLoS one

Screening of *MAMLD1* Mutations in 70 Children with 46,XY DSD: Identification and Functional Analysis of Two New Mutations

Nicolas Kalfa[1,2], Maki Fukami[3], Pascal Philibert[1], Francoise Audran[1], Catherine Pienkowski[4], Jacques Weill[5], Graziella Pinto[6], Sylvie Manouvrier[7], Michel Polak[6], Totsumo Ogata[3], Charles Sultan[1,2,8]*

1 Service d'Hormonologie, Hôpital Lapeyronie, CHU de Montpellier et UM1, Montpellier, France, **2** Service de Chirurgie et Urologie Pédiatrique, Hôpital Lapeyronie, CHU de Montpellier et UM1, Montpellier, France, **3** Department of Molecular Endocrinology, National Research Institute for Child Health and Development, Tokyo, Japan, **4** Unité d'Endocrinologie Pédiatrique, Hôpital des Enfants, CHU de Toulouse, Toulouse, France, **5** Clinique de Pédiatrie, Hôpital Jeanne de Flandre, CHU de Lille, Lille, France, **6** Unité d'Endocrinologie Pédiatrique, Hôpital Necker Enfants Malades, APHP, Paris, France, **7** Service de Génétique Clinique, Hôpital Jeanne de Flandre, CHU de Lille, Lille, France, **8** Unité d'Endocrinologie et Gynécologie Pédiatriques, Service de Pédiatrie, Hôpital Arnaud de Villeneuve et UM1, CHU de Montpellier, Montpellier, France

Abstract

More than 50% of children with severe 46,XY disorders of sex development (DSD) do not have a definitive etiological diagnosis. Besides gonadal dysgenesis, defects in androgen biosynthesis, and abnormalities in androgen sensitivity, the Mastermind-like domain containing 1 (*MAMLD1*) gene, which was identified as critical for the development of male genitalia, may be implicated. The present study investigated whether *MAMLD1* is implicated in cases of severe 46,XY DSD and whether routine sequencing of *MAMLD1* should be performed in these patients. Seventy children with severe non-syndromic 46,XY DSD of unknown etiology were studied. One hundred and fifty healthy individuals were included as controls. Direct sequencing of the *MAMLD1, AR, SRD5A2* and *NR5A1* genes was performed. The transactivation function of the variant *MAMLD1* proteins was quantified by the luciferase method. Two new mutations were identified: p.S143X (c.428C>A) in a patient with scrotal hypospadias with microphallus and p.P384L (c.1151C>T) in a patient with penile hypospadias with microphallus. The *in vitro* functional study confirmed no residual transactivating function of the p.S143X mutant and a significantly reduced transactivation function of the p.P384L protein ($p = 0.0032$). The p.P359S, p.N662S and p.H347Q variants are also reported with particularly high frequency of the p.359T- p.662G haplotype in the DSD patients. Severe undervirilization in XY newborns can reveal mutations of *MAMLD1*. *MAMLD1* should be routinely sequenced in these patients with otherwise normal *AR, SRD5A2* and *NR5A1*genes.

Citation: Kalfa N, Fukami M, Philibert P, Audran F, Pienkowski C, et al. (2012) Screening of *MAMLD1* Mutations in 70 Children with 46,XY DSD: Identification and Functional Analysis of Two New Mutations. PLoS ONE 7(3): e32505. doi:10.1371/journal.pone.0032505

Editor: Irina Agoulnik, Florida International University, United States of America

Received November 7, 2011; **Accepted** January 31, 2012; **Published** March 30, 2012

Funding: This study was funded by a Programme Hospitalier de Recherch Clinique Inter-Régional (PHRC number UF 8270) provided by CHU de Montpellier and by a grant from Fondation pour la Recherche Médicale FRM110309. The funders had no role in study design, data collection and analysis, decision to publish, or preparation of the manuscript.

Competing Interests: The authors have declared that no competing interests exist.

* E-mail: c-sultan@chu-montpellier.fr

Introduction

The disorders of sex development (DSD) comprise a variety of anomalies defined by congenital conditions in which chromosomal, gonadal, or anatomical sex is atypical. The prevalence of the 46,XY disorders of sex development (46,XY DSD) is difficult to determine with accuracy because of the heterogeneity in the clinical presentation and the etiologies. The estimated incidence of severe 46,XY DSD with uncertain sex is 2.2 per 10,000 births [1], and for a minor form of 46,XY DSD with isolated and non-severe hypospadias, the incidence is estimated at 1 in 250–400 births [2]. Two independent surveillance systems in the United States, the nationwide Birth Defects Monitoring Program (BDMP) and the Metropolitan Atlanta Congenital Defects Program (MACDP), reported a near doubling in the hypospadias rate in comparison with the immediately preceding decades [3]. Although recent studies have questioned this reported rise and provide conflicting data [4,5], the elucidation of the pathophysiology of these genital malformations remains challenging.

The etiologies of 46,XY DSD are usually gonadal dysgenesis (defect in *SRY* and downstream genes such as *SOX9, WT1, NR5A1* [6,7], etc.), defects in androgen biosynthesis and, more frequently, abnormalities in androgen sensitivity. Unfortunately, more than 50% of children with severe 46,XY DSD presenting with uncertain sex do not have a definitive clinical diagnosis [8]. For instance, an *AR* gene defect is identified in less than 10% of the cases [9].

In addition to these well classified causes, a recent candidate gene was identified as critical for the development of male genitalia: the Mastermind-like domain containing 1 (*MAMLD1*) gene (formerly *CXorf6*). This gene was discovered during studies to find the gene responsible for X-linked myotubular myopathy, *MTM1*, which maps to proximal Xq28 [10]: *MAMLD1* was observed to be deleted in patients with both the myopathy and external genital malformations [10,11,12]. Polymorphisms of *MAMLD1* have been reported in patients with isolated hypospadias, the less severe form of 46,XY DSD, but these variants usually

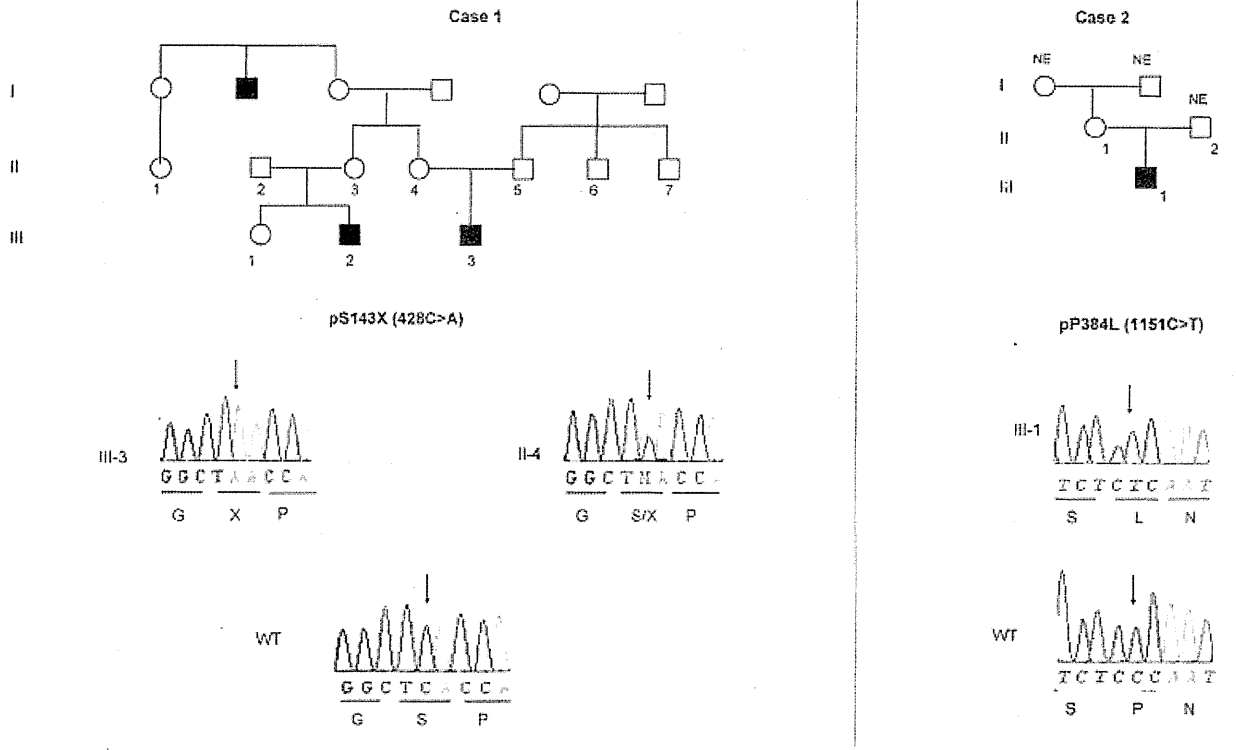

Figure 1. Electrochromatograms and pedigrees of the three patients with *MAMLD1* mutations. The black squares indicate patients with posterior hypospadias. All mutant sequences were controlled by wildtype (WT) DNA. Regarding case 1's family, only the members III-3 and II-4 were genotyped, as the other members in the pedigree declined genetic testing.
doi:10.1371/journal.pone.0032505.g001

do not affect the transactivation of the protein [13,14]. Conversely, severe 46,XY DSD with uncertain sex has been sparsely studied. To date, only one study has focused on these patients: Fukami et al. identified three nonsense mutations in four individuals from a group of 166 patients [15]. The aim of the present study was to determine whether *MAMLD1* is frequently implicated in newborns and children with severe 46,XY DSD with uncertain sex and whether *MAMLD1* should be routinely sequenced in these patients.

Materials and Methods

Patients and controls

Two hundred and twenty individuals were included in this study. Seventy children presented with non-syndromic 46,XY DSD of unknown etiology. According to the Quigley classification [16], 8 patients exhibited a stage 2 phenotype; 32 patients, stage 3; 20 patients, stage 4; 5 patients, stage 5; and 5 patients, stage 6. One hundred and fifty healthy individuals were included as controls. Controls were chosen among patients without urinary, genital, or endocrine disease, or any other congenital malformation. For instance, patients with acute appendicitis or operated on for circumcision without phimosis were included. This study was approved by the Institutional Review Board (CPP-Montpellier, ID RCB No. 2008-A00781-54). Written consent was obtained from the parents, carers or guardians on behalf of the participating minors. When a mutation was identified, other family members were examined if possible. The patients and controls were Caucasian.

DNA extraction

DNA was extracted from peripheral blood using a QIAamp DNA blood minikit (Qiagen, Courtaboeuf, France).

Mutational analysis of MAMLD1

Direct sequencing of *MAMLD1* coding exons and their flanking splice sites was performed in all patients and controls using primers as previously described [17]. The 3730xl DNA Analyzer (Applied Biosystems, Foster City, CA, USA) was used. Sequencing reactions were repeated twice with at least two different PCR products. The DNA sequences were compared with the sequences of normal controls and the reference genomes from the ensembl.org database (Ensembl: ENSG00000013619) and the genebank database (MIM: 300120, NCBI Gene ID: 10046). It is notable that the number of the cDNA and amino acids has been changed recently because of the recognition of a novel *MAMLD1* start codon. This report describes *MAMLD1* cDNA and amino acids according to the new system.

Molecular analysis of androgen sensitivity

A molecular analysis of the androgen receptor (*AR*) and 5 alpha reductase type 2 (*SRD5A2*) genes was performed in all patients.

Table 1. Clinical and hormonal data of patients with mutated *MAMLD1*.

Patient	Case 1	Case 2
MAMLD1 mutation	pS143X	pP384L
Previous medical history	None	Maternal diabetes
Genital phenotype		
Urethral meatus	Scrotal	Penile posterior
Age at exam (yr,mo)	0,0	0,0
Microphallus	Yes, 20 mm	Yes, 20 mm with cuvature
Testis position	Intra-scrotal	Intra-scrotal
Testis size (normal = 1–2 ml)	Normal	Normal
Scrotal appearance	Ventral transposition, Bifid Scrotum	Bifid Scrotum
Renal and urinary tract structure	Normal	Normal
Extragenital phenotype	Normal	Normal
Growth		
Birth height, cm (SDS)	51 (+0)	50.5 (+0)
Birth weight, Kg (SDS)	3.540 (+0)	3.750 (+0.5)
Serum hormone level		
Time of measurment (yr,mo)	0,0	0,3
Testosterone (ng/ml) (1–3 ng/ml)	1.78	<0.07
LH (UI/l) (1–12 UI/l)	10	0.3
FSH (UI/l) (1–10 UI/l)	0.8	0.8
AMH	336 ng/ml	19 ng/ml*
Inhibin	NA	<15 ng/ml*

SD: standard deviation. ND: not determined. NA: not available. DHT: dihydrotestosterone. DHEA: dihydroepiandrsosterone. Parentheses indicate the standard deviation for height and weight and the normal range for hormone serum levels. Testes of 1–2 ml can be regarded as normal, as recently reported by Shibata et al. [34].
*It is notable that anti-mullerian hormone and inhibin were lowered in one case. *MAMLD1* is indeed reported to be expressed in Sertoli cells, as well [15].
doi:10.1371/journal.pone.0032505.t001

Exons 1–8 of the *AR* gene were amplified by PCR using sets of primers and reactions previously described [18]. Molecular analysis of the *SRD5A2* gene (exons 1–5) was performed as previously reported [19]. PCRs were verified for correct length on agarose gel, purified with Qiaquick PCR columns (Qiagen), and sequenced with the ABI Prism Big Dye terminator sequencing kit. *NR5A1*was sequenced in 46,XY DSD children with low plasma testosterone as previously published [6,20].

Homology study

Ensembl.org detected the putative homologs of the human *MAMLD1* gene and alignments were made with the ClustalW software at http://www.ebi.ac.uk/Tools/msa/clustalw2/.

Structure prediction

The potential impact of variants was first predicted using X *in-silico* tools for secondary structure, tertiary structure and prediction of the consequences of amino acid changes.

The secondary structure for wildtype and variants was predicted using JPred software [21] (http://www.compbio.dundee.ac.uk/www-jpred/). The relative accessibility of amino acids was studied with Netsurf software [22] (http://www.cbs.dtu.dk/services/NetSurfP/). The three-dimensional structure was predicted by the Protein Homology/analogY Recognition Engine (PhyreEngine) from the Structural Bioinformatics Group, Imperial College, London, at http:www.sbg.bio.ic.ac.uk/phyrew/. This tool can detect remote homologous proteins with similar tertiary structures, based on multiple sequence profiles with structure-based profiles [23].

The functional consequences of amino acid changes were predicted using four algorithms. Polyphen (Harvard, USA) [24,25], Panther [26], Sift (University of British Columbia) [27] and SNP-3D (University of Maryland) [28] were used, respectively, at http://genetics.bwh.harvard.edu/pph/, http://www.pantherdb.org/tools/csnpScoreForm.jsp., http://sift.jcvi.org/, and http://www.snps3d.org/modules.php?name=Search&op=advanced%20search. These algorithms are based on the alignment of orthologous and/or paralogous protein sequences and/or structural constraints.

Transactivation analysis of MAMLD1

The transactivation function of the variant MAMLD1 proteins was analyzed by the luciferase method [29]. We used the previously reported luciferase reporter vector containing the promoter sequence of mouse hairy/enhancer of split 3 (*Hes3*) (−2,715~+261 bp) [30] and expression vectors containing cDNAs for wildtype *MAMLD1*, p.S143X and p.P384L [29]. Mouse Leydig tumor (MLTC1) cells (ATCC, CRL-2065) seeded in 12-well dishes ($0.5–1.0\times10^5$ cells/well) were transiently transfected using Lipofectamine 2000 (Invitrogen) with 0.6 μg of luciferase reporter vector and 0.6 μg of expression vector for wildtype or variant *MAMLD1*, together with 20 ng of pRL-CMV vector (Promega) used as an internal control. As a control for the expression vectors, an empty counterpart vector was transfected. Luciferase assays performed with a Lumat LB9507 (Berthold) 48 hours after transfection were repeated three times.

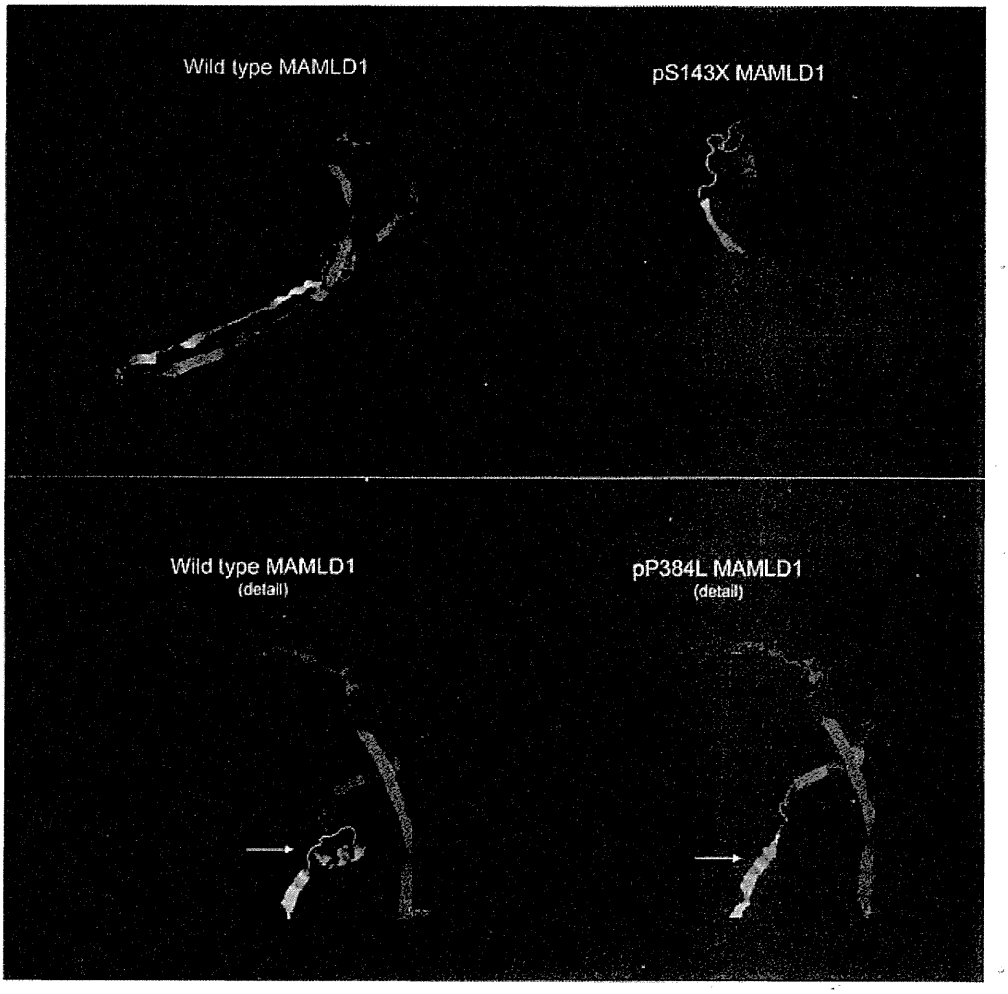

Figure 2. Tertiary structure prediction of the wildtype protein (left column) and with the mutants. 3D structure was predicted at Protein Homology/analogY Recognition Engine (PhyreEngine) from the Structural Bioinformatics Group, Imperial College, London, at http:www.sbg.bio.ic.ac.uk/phyre~/. The plain arrows show the changes in the shape of the protein between the wildtype and p.P384L.
doi:10.1371/journal.pone.0032505.g002

Statistical methods

Haplotype frequencies were compared between cases and controls using the χ^2 test and the Fisher test on SPSS 16.0 software. The odds ratio (OR) was also considered with the logit confidence intervals method: $OR-CI=e^{LN(OR)\pm 1.96\left(\frac{1}{A}+\frac{1}{B}+\frac{1}{C}+\frac{1}{D}\right)^{0.5}}$. Hapmap and ensembl.org were used to exclude linkage disequilibrium. Regarding the transactivation analysis of *MAMLD1*, the results are expressed using the mean and SD, and statistical significance was determined by the *t*-test.

Results

Mutations of MAMLD1 and functional analyses

Among the 70 newborns and children with 46,XY DSD, two new mutations were identified in two unrelated patients: p.S143X (c.428C>A) and p.P384L (c.1151C>T) (Fig. 1). The clinical and genetic data are summarized in Table 1. None of these mutations was noted in the control group. The sequences of the *AR*, *SRD5A2* and *NR5A1* genes were normal in these patients.

a- The p.S143X mutation was predicted to cause a short and truncated protein. The *in silico* prediction showed profoundly modified amino acid accessibility and 3D structure. Relative surface accessibility and absolute surface accessibility of the last amino acid changed from 0.248 to 0.834 and from 29.124 to 97.721, respectively. PhyreEngine predicted the loss of any functional site without a residual consensus sequence (no homologous sequence over 5% through whole genome) (Fig. 2). The *in vitro* functional study confirmed no residual transactivating function of the mutant (Fig. 3). Interestingly, a maternal uncle and a maternal cousin of the index case both exhibited severe hypospadias (not available for genetic testing). The mother was indeed heterozygous for the mutation (Fig. 1).

b- The p.P384L mutation was found in a patient with posterior penile hypospadias and microphallus. No cryptochidism was noted. The secondary structure was predicted to be changed in the next four amino acids. The relative and absolute accessibilities of the amino acid were modified from 0.27 to 0.35 and from 39.07 to 65.25, respectively. The 3D structure prediction of the mutated protein was significantly changed (Fig. 2). All four *in silico*

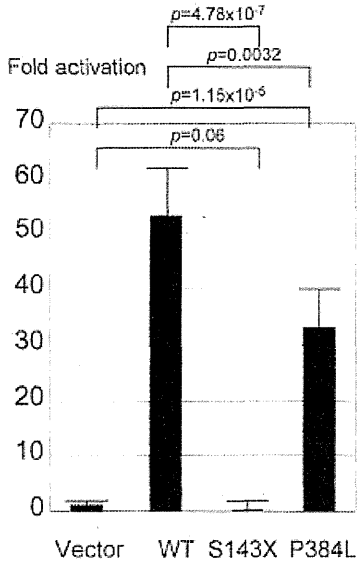

Figure 3. Transactivation function of the variants of the MAMLD1 protein analyzed by the luciferase method. The activity is evaluated for pHes3-luc vector.
doi:10.1371/journal.pone.0032505.g003

algorithms predicted affected protein function (Table 2) with a conserved amino acid throughout species (Table 3). Functional studies confirmed the significantly reduced transactivation function of the p.P384L protein with 60% residual activity when compared with the wildtype protein, $p = 0.0032$ (Fig. 3).

Polymorphisms of MAMLD1

We identified three polymorphisms of *MAMLD1* in our series: p.P359S (c.1075C>T, rs41313406), p.N662S (c.1985A>G, rs2073043) and p.H347Q (c.1041C>A, rs62641609). Regarding the p.P359S and p.N662S polymorphisms, 14 patients exhibited double polymorphisms (S-S haplotype) and five had the p.N359S polymorphism. The phenotypes of the patients with the S-S haplotype were as follows: penile posterior hypospadias and cryptorchidism in three cases, hypospadias and microphallus in five cases (anterior n = 1, penile posterior n = 2 and scrotal hypospadias n = 2), and cryptorchidism and microphallus in six cases (bilateral cryptorchidism n = 5, unilateral cryptorchidism n = 1). Using hapmap and ensembl.org, no linkage disequilibrium was found for these two variants. In previous studies, we and others found that the S-S haplotype was present in only 6/150 controls (4.0%) and 23/360 controls (6.4%) [13,14]. By combining the published series for controls (matched patients and controls), we determined that the incidence of the S-S haplotype was higher in the DSD patients (20%, n = 70 vs. 6%, n = 510, $p = 0.0003$) (OR = 3.86, CI from 1.94 to 7.70, $p = 0.05$). Haplotypes and their relative frequencies in each group of patients are summarized in Table 4.

The p.H347Q variant, previously reported as a polymorphism especially in sub-Saharan populations (rs62641609, http://www.ensembl.org/Homo_sapiens/Variation/Summary?r=X:149638386-149639386;v=rs62641609;vdb=variation;vf=16740729), was identified in a patient with posterior hypospadias and microphallus (25 mm length at birth).

Table 2. Prediction of affected protein function using four algorithms.

Algorithm	pP384L
Polyphen	Probably damaging
	score = 0.961 (sensitivity: 0.71; specificity: 0.93)
Sift	Affect protein function
	Sift score = 0.04
Panther	Probability of deleterious effect = 0.42
	(subPSEC score = −2.7)
SNPS3D	Deleterious
	(svm score = −1.75)

References and online access are indicated in the text. Mathematical calculation of the significance of each score is available online.
doi:10.1371/journal.pone.0032505.t002

Discussion

MAMLD1 is a good candidate to explore in patients with unexplained 46,XY DSD, as it has been shown to be expressed in fetal Leydig cells around the critical period for sex development [15]. The transient knockdown of *MAMLD1* mRNA expression results in significantly reduced testosterone production in mouse Leydig tumor cells [29]. *MAMLD1* is further coexpressed with steroidogenic factor (*NR5A1*), which regulates the transcription of genes involved in sex development, and an *NR5A1*target site was found within the *MAMLD1* gene [29,31]. *MAMLD1* thus seems to have an important role in modulating testosterone production during sex development and is involved in the 46,XY disorders of sex development [32].

Regarding the minor forms of 46,XY DSD with isolated and non-severe hypospadias, mutational studies of *MAMLD1* have identified several polymorphisms in this gene. We reported the following variants in patients with isolated hypospadias: p.P359S, p.V505A, p.N662S and p.604ins3Q [13,17], all of which were recently confirmed as polymorphisms [14]. The p.Q602K mutation was also found in one patient with posterior hypospadias and was predicted to affect the splicing process. An association between isolated hypospadias and the rare haplotype p.P359S-p.N662S is also suspected [13,14].

Table 3. Homology study showed that this amino acid was highly conserved through species for the c.1041C>A and c.1151C>T mutations.

Patient	MSSNTLSGSTLRGS**L**NALLSSMTSSSNAAL
Human-MAMLD1	MSSNTLSGSTLRGS**P**NALLSSMTSSSNAAL
Pig	MSSSSLPGSTLHGS**P**GALLSSGAPSSSSAL
Horse	MSSSNLPGSTLQGS**P**NALLSSMVSGSSAAL
Chimpanzee	MSSNTLSGSTLRGS**P**NALLSSMTSSSNAAL
Mouse	MSSSSLSGSAVQSS**P**NALLSSMAPSSNASL
Rabbit	MAPHSLPGSSLQGS**P**NALLSSMAPNSSGAL
Dog	MASSNLPGSSFQAS**P**NALLASMASASSSAGL
Cat	MASGNLPGSAFQGS**P**NALLASMASGSSAAL

doi:10.1371/journal.pone.0032505.t003

Table 4. Incidence of exonic polymorphisms p.P359S and p.N662S, and relative haplotypes in normal controls and 46,XY DSD patients.

Haplotype 359-662	Patients, n = 70	Controls, n = 510	Fisher, p value	OR	OR confidence interval (p = 0.05)
p.359C- p.662A	72.9% (n = 51)	90.6% (n = 462)	p = 0.0001	0.28	0.15–0.51
p.359T- p.662A	0%	1.5% (n = 8)	p = 0.60	0.42	0.02–7.35
p.359C- p.662G	7.1% (n = 5)	0.8% (n = 9)	p = 0.02	4.28	1.39–13.17
p.359T- p.662G (S-S polymorphism)	20% (n = 14)	6% (n = 31)	p = 0.0003	3.86	1.94–7.70

Controls are combined with the published series (matched for ethnicity of patients and controls) [13] [14]. The χ-square test was performed. When combining all patients with the p.662G polymorphism whatever the p.359 allele, this p.662G was significantly more frequent in 46,XY DSD patients: 27.1% (n = 19) vs. 6.8% (n = 40), $p = 0.0001$.

doi:10.1371/journal.pone.0032505.t004

Regarding severe 46,XY DSD with uncertain sex, only one published paper to date has reported three *MAMLD1* mutations (p.E124X, p.Q197X and p.R653X) [15]. It is precisely in this situation of severe genital malformation that the diagnosis of the causative mechanism is of clinical interest for medical treatment (hormone substitution, pubertal follow-up). In order to determine whether this report was an exceptional observation or of practical clinical interest, we screened 70 patients with severe 46,XY DSD of unknown origin. We identified two new mutations of *MAMLD1* in patients with severe hypospadias and microphallus (1 stop codon and 1 missense mutation). These mutations were associated with a severe phenotype, and reduced (p.P384L) or abolished (p.S143X) transactivation function was found in two cases. 46,XY DSD with normal *AR*, *SRD5A2* and *NR5A1*gene sequences can thus reveal a mutation of *MAMLD1*. This finding suggests a new diagnostic investigation for these patients and may be helpful in genetic counselling if a mutation is identified. It also provides new insight into the pathophysiology of DSD. Indeed, in the family of the child bearing the p.S143X mutation, the mother was heterozygous and two other males on the maternal side of the family exhibited a consistent phenotype. Unfortunately, the family declined any further investigation.

The mechanisms by which these mutations with reduced transactivation induce DSD are still under investigation. As noted above, several studies have provided strong evidence of *MAMLD1* implication in fetal sex development through modulation of testosterone production at the time of sex differentiation. The plasma testosterone measured in one of our cases was indeed lowered but it was normal in the other one, as previously reported in patients with nonsense mutations [15]. Plasma testosterone evaluation is thus not systematically helpful in orienting the diagnosis of DSD since mutations of the genes implicated in testosterone production - such as *MAMLD1* and *NR5A1* - have been reported in 46,XY DSD patients with normal plasma testosterone. These findings, along with the absence of correlation between the *in vitro* functional analysis and the biological and clinical phenotype, suggest that the genital malformation is primarily related to a transient prenatal testicular (Leydig cell) dysfunction and the resulting compromised testosterone production around the critical period of sex differentiation [33]. In the postnatal period, the mouse homolog of *MAMLD1* was indeed reported to be weakly expressed in the testis at one week of age and the expression was faint thereafter.

We also report a high incidence of the rare haplotype p.P359S-p.N662S in our series. The p.P359S (which was designated p.P286S in the previous report) variant was first reported in a patient with hypospadias but it was absent in his brother and nephew with the same phenotype [15]. The p.N662S (which was designated p.P589S in the previous report) variant was found in hypospadiac patients but was also reported in a normal population, although with low incidence [15]. We and others have found that the S-S haplotype is associated with a minor form of DSD, i.e., isolated hypospadias [14], but the *in vitro* functional study of the p.P359S-p.N662S *MAMLD1* variant was inconclusive with unchanged transactivation function [13]. In the present study, we show that the combination of these alleles was present in as much as 15% of patients with severe 46,XY DSD. This is significantly higher than in the controls [combining the series, 15% (n = 70) vs. 10.7% (n = 510), $p = 0.0003$]. Again, a transient testosterone production failure during prenatal development may have contributed to the undervirilization of the external genitalia, but how this haplotype can be present in normal, mild and severe phenotypes remains to be elucidated.

Severe undervirilization in XY newborns can reveal mutations of *MAMLD1*. *MAMLD1* should be routinely sequenced in these patients with otherwise normal *AR*, *SRD5A2* and *NR5A1* genes.

Acknowledgments

We would like to thank Dr Bérond (Laboratoire de Génétique Chromosomique, Institut Universitaire de Recherche Clinique, Université de Montpellier 1, France) for his great help in the statistical study of haplotypes.

Author Contributions

Conceived and designed the experiments: NK MF CS TO PP. Performed the experiments: NK MF PP FA. Analyzed the data: NK MF PP FA CP JW GP SM MP. Contributed reagents/materials/analysis tools: CP JW GP SM MP. Wrote the paper: NK TO CS PP FA.

References

1. Thyen U, Lanz K, Holterhus PM, Hiort O (2006) Epidemiology and initial management of ambiguous genitalia at birth in Germany. Horm Res 66: 195–203.
2. Nelson P (2007) Epidemiology of Hypospadias. Dialogues in Pediatric Urology 28: 2–3.
3. Paulozzi LJ, Erickson JD, Jackson RJ (1997) Hypospadias trends in two US surveillance systems. Pediatrics 100: 831–834.
4. Martinez-Frias ML, Prieto D, Prieto L, Bermejo E, Rodriguez-Pinilla E, et al. (2004) Secular decreasing trend of the frequency of hypospadias among newborn male infants in Spain. Birth Defects Res A Clin Mol Teratol 70: 75–81.
5. Fisch H, Hyun G, Hensle TW (2010) Rising hypospadias rates: disproving a myth. J Pediatr Urol 6: 37–39.
6. Lin L, Philibert P, Ferraz-de-Souza B, Kelberman D, Homfray T, et al. (2007) Heterozygous missense mutations in steroidogenic factor 1 (SF1/Ad4BP,

NR5A1) are associated with 46,XY disorders of sex development with normal adrenal function. J Clin Endocrinol Metab 92: 991–999.
7. Coutant R, Mallet D, Lahlou N, Bouhours-Nouet N, Guichet A, et al. (2007) Heterozygous mutation of steroidogenic factor-1 in 46,XY subjects may mimic partial androgen insensitivity syndrome. J Clin Endocrinol Metab 92: 2868–2873.
8. Morel Y, Rey R, Teinturier C, Nicolino M, Michel-Calemard L, et al. (2002) Aetiological diagnosis of male sex ambiguity: a collaborative study. Eur J Pediatr 161: 49–59.
9. Choi J, Kim G, Seo E, KS K, Kim S, et al. (2008) Molecular analysis of the AR and SRD5A2 genes in patients with 46,XY disorders of sex development. J Pediatr Endocrinol Metab 21: 545–553.
10. Laporte J, Kioschis P, Hu LJ, Kretz C, Carlsson B, et al. (1997) Cloning and characterization of an alternatively spliced gene in proximal Xq28 deleted in two patients with intersexual genitalia and myotubular myopathy. Genomics 41: 458–462.
11. Bartsch O, Kress W, Wagner A, Seemanova E (1999) The novel contiguous gene syndrome of myotubular myopathy (MTM1), male hypogenitalism and deletion in Xq28:report of the first familial case. Cytogenet Cell Genet 85: 310–314.
12. Hu LJ, Laporte J, Kress W, Kioschis P, Siebenhaar R, et al. (1996) Deletions in Xq28 in two boys with myotubular myopathy and abnormal genital development define a new contiguous gene syndrome in a 430 kb region. Hum Mol Genet 5: 139–143.
13. Kalfa N, Cassorla F, Audran F, Oulad Abdennabi I, Philibert P, et al. (2011) Polymorphisms of MAMLD1 gene in hypospadias. J Pediatr Urol 7: 585–591.
14. Chen Y, Thai HT, Lundin J, Lagerstedt-Robinson K, Zhao S, et al. (2010) Mutational study of the MAMLD1-gene in hypospadias. Eur J Med Genet 53: 122–126.
15. Fukami M, Wada Y, Miyabayashi K, Nishino I, Hasegawa T, et al. (2006) CXorf6 is a causative gene for hypospadias. Nat Genet 38: 1369–1371.
16. Quigley CA, French FS (1994) Androgen insensitivity syndromes. Curr Ther Endocrinol Metab 5: 342–351.
17. Kalfa N, Lin B, Ophir K, Audran F, Wang MH, et al. (2008) Mutations of CXorf6 are associated with a range of severities of hypospadias. Eur J Endocrinol 159: 453–458.
18. Philibert P, Audran F, Pienkowski C, Morange I, Kohler B, et al. (2010) Complete androgen insensitivity syndrome is frequently due to premature stop codons in exon 1 of the androgen receptor gene: an international collaborative report of 13 new mutations. Fertil Steril 94: 472–476.
19. Maimoun L, Philibert P, Cammas B, Audran F, Bouchard P, et al. (2010) Phenotypical, Biological, and Molecular Heterogeneity of 5{alpha}-Reductase Deficiency: An Extensive International Experience of 55 Patients. J Clin Endocrinol Metab 96: 296–307.
20. Philibert P, Lepricur E, Zenaty D, Thibaud E, Polak M, et al. (2010) Steroidogenic factor-1 (SF-1) gene mutation as a frequent cause of primary amenorrhea in 46,XY female adolescents with low testosterone concentration. Reprod Biol Endocrinol 8: 28.
21. Cole C, Barber JD, Barton GJ (2008) The Jpred 3 secondary structure prediction server. Nucleic Acids Res 36: W197–201.
22. Petersen B, Petersen TN, Andersen P, Nielsen M, Lundegaard C (2009) A generic method for assignment of reliability scores applied to solvent accessibility predictions. BMC Struct Biol 9: 51.
23. Kelley LA, Sternberg MJ (2009) Protein structure prediction on the Web: a case study using the Phyre server. Nat Protoc 4: 363–371.
24. Ramensky V, Bork P, Sunyaev S (2002) Human non-synonymous SNPs: server and survey. Nucleic Acids Res 30: 3894–3900.
25. Thomas PD, Kejariwal A (2004) Coding single-nucleotide polymorphisms associated with complex vs. Mendelian disease: evolutionary evidence for differences in molecular effects. Proc Natl Acad Sci U S A 101: 15398–15403.
26. Mi H, Dong Q, Muruganujan A, Gaudet P, Lewis S, et al. (2010) PANTHER version 7: improved phylogenetic trees, orthologs and collaboration with the Gene Ontology Consortium. Nucleic Acids Res 38: D204–210.
27. Kumar P, Henikoff S, Ng PC (2009) Predicting the effects of coding non-synonymous variants on protein function using the SIFT algorithm. Nat Protoc 4: 1073–1081.
28. Yue P, Melamud E, Moult J (2006) SNPs3D: candidate gene and SNP selection for association studies. BMC Bioinformatics 7: 166.
29. Fukami M, Wada Y, Okada M, Kato F, Katsumata N, et al. (2008) Mastermind-like domain containing 1 (MAMLD1 or CXorf6) transactivates the Hes3 promoter, augments testosterone production, and contains the SF1 target sequence. J Biol Chem 29: 5525–5532.
30. Nishimura M, Isaka F, Ishibashi M, Tomita K, Tsuda H, et al. (1998) Structure, chromosomal locus, and promoter of mouse Hes2 gene, a homologue of Drosophila hairy and Enhancer of split. Genomics 49: 69–75.
31. Sadovsky Y, Dorn C (2000) Function of steroidogenic factor 1 during development and differentiation of the reproductive system. Rev Reprod 5: 136–142.
32. Ogata T, Laporte J, Fukami M (2009) MAMLD1 (CXorf6): a new gene involved in hypospadias. Horm Res 71: 245–252.
33. Welsh M, MacLeod DJ, Walker M, Smith LB, Sharpe RM (2010) Critical androgen-sensitive periods of rat penis and clitoris development. Int J Androl 33: e144–152.
34. Shibata Y, Kojima Y, Mizuno K, Nakane A, Kato T, et al. Optimal cutoff value of contralateral testicular size for prediction of absent testis in Japanese boys with nonpalpable testis. Urology 76: 78–81.

OPEN ACCESS Freely available online

PLoS one

Identification of Novel Low-Dose Bisphenol A Targets in Human Foreskin Fibroblast Cells Derived from Hypospadias Patients

Xian-Yang Qin[1,2], Yoshiyuki Kojima[3], Kentaro Mizuno[3], Katsuhiko Ueoka[4], Koji Muroya[5], Mami Miyado[6], Hiroko Zaha[1], Hiromi Akanuma[1], Qin Zeng[1], Tomokazu Fukuda[7], Jun Yoshinaga[2], Junzo Yonemoto[1], Kenjiro Kohri[3], Yutaro Hayashi[3], Maki Fukami[6], Tsutomu Ogata[6,8], Hideko Sone[1]*

1 Health Risk Research Section, Research Center for Environmental Risk, National Institute for Environmental Studies, Tsukuba, Ibaraki, Japan, **2** Department of Environmental Studies, Graduate School of Frontier Science, The University of Tokyo, Kashiwa, Chiba, Japan, **3** Department of Nephro-Urology, Nagoya City University Graduate School of Medical Sciences, Nagoya, Aichi, Japan, **4** Department of Surgical Subspecialties, National Research Center for Child Health and Development, Tokyo, Japan, **5** Division of Endocrinology and Metabolism, Kanagawa Children's Medical Center, Kanagawa, Yokohama, Japan, **6** Department of Endocrinology and Metabolism, National Research Institute for Child Health and Development, Tokyo, Japan, **7** Department of Animal Production Science, Graduate School of Agricultural Science, Tohoku University, Sendai, Miyagi, Japan, **8** Department of Pediatrics, University Hospital, Hamamatsu University School of Medicine, Hamamatsu, Shizuoka, Japan

Abstract

Background/Purpose: The effect of low-dose bisphenol A (BPA) exposure on human reproductive health is still controversial. To better understand the molecular basis of the effect of BPA on human reproductive health, a genome-wide screen was performed using human foreskin fibroblast cells (hFFCs) derived from child hypospadias (HS) patients to identify novel targets of low-dose BPA exposure.

Methodology/Principal Findings: Gene expression profiles of hFFCs were measured after exposure to 10 nM BPA, 0.01 nM 17β-estradiol (E2) or 1 nM 2,3,7,8-tetrachlorodibenzo-p-dioxin (TCDD) for 24 h. Differentially expressed genes were identified using an unpaired Student's t test with *P* value cut off at 0.05 and fold change of more than 1.2. These genes were selected for network generation and pathway analysis using Ingenuity Pathways Analysis, Pathway Express and KegArray. Seventy-one genes (42 downregulated and 29 upregulated) were identified as significantly differentially expressed in response to BPA, among which 43 genes were found to be affected exclusively by BPA compared with E2 and TCDD. Of particular interest, real-time PCR analysis revealed that the expression of matrix metallopeptidase 11 (MMP11), a well-known effector of development and normal physiology, was found to be inhibited by BPA (0.47-fold and 0.37-fold at 10 nM and 100 nM, respectively). Furthermore, study of hFFCs derived from HS and cryptorchidism (CO) patients ($n = 23$ and 11, respectively) indicated that MMP11 expression was significantly lower in the HS group than in the CO group (0.25-fold, $P = 0.0027$).

Conclusions/Significance: This present study suggests that an involvement of BPA in the etiology of HS might be associated with the downregulation of MMP11. Further study to elucidate the function of the novel target genes identified in this study during genital tubercle development might increase our knowledge of the effects of low-dose BPA exposure on human reproductive health.

Citation: Qin X-Y, Kojima Y, Mizuno K, Ueoka K, Muroya K, et al. (2012) Identification of Novel Low-Dose Bisphenol A Targets in Human Foreskin Fibroblast Cells Derived from Hypospadias Patients. PLoS ONE 7(5): e36711. doi:10.1371/journal.pone.0036711

Editor: Bin He, Baylor College of Medicine, United States of America

Received March 6, 2012; **Accepted** April 12, 2012; **Published** May 4, 2012

Funding: This study was supported by the Ministry of the Environment, Japan, and by a grant for Research on Risk on Chemical Substances (H20-004) from the Ministry of Health, Labour and Welfare, Japan (http://www.mhlw.go.jp/english/index.html). The funders had no role in the study design, data collection and analysis, decision to publish, or preparation of the manuscript.

Competing Interests: The authors have declared that no competing interests exist.

* E-mail: hsone@nies.go.jp

Introduction

Hypospadias (HS) is one of the most common congenital abnormalities with a global prevalence of approximately 0.2–1% at birth in male infants [1]. The etiology of HS is poorly understood, and might include genetic, hormonal and environmental factors. It has been hypothesized that testicular cancer, cryptorchidism (CO) and some cases of HS and impaired spermatogenesis are symptoms of a single underlying entity that has been named as the testicular dysgenesis syndrome (TDS) [2,3]. This concept proposes the existence of a common underlying cause for the occurrence of these reproductive and developmental diseases, and suggests that adverse environmental factors, such as environmental endocrine disruptors (EEDs) might exert their etiological effects on a susceptible genetic background.

Bisphenol A (BPA) is one of the world's highest production-volume chemicals, with more than six billion pounds produced worldwide each year [4]. BPA is used extensively in the plastics produced for food and beverage containers, such as baby bottles,

plastic containers and the resin lining of cans [4]. Among the known estrogen-like EEDs, BPA has received much attention because it is commonly found in the environment as well as in human tissues and fluids (1–19.4 nM) [4,5]. BPA has been detected in 92% of urine samples in a US reference population, suggesting people may be continuously exposed to this compound in their daily lives [6]. The US Food and Drug Administration and Environmental Protection Agency concluded in the 1980s that a daily dose of 50 μg/kg/day was safe for humans, which is currently considered as $<2.19\times10^{-7}$ M for *in vitro* cell or organ culture studies [7]. However, in recent decades, there has been a heated controversy over the safety of BPA among scientists and risk assessors.

Recently, exposure to BPA at concentrations detected in humans has been reported to affect neurological, cardiovascular and metabolic diseases (such as diabetes), and even cancers [8–12]. However, the effect of low-dose BPA exposure on human reproductive health is still controversial [13,14]. Li *et al.* reported that occupational exposure to BPA has adverse effects on male sexual dysfunction, which is the first evidence that exposure to BPA in the workplace could have an adverse effect on male sexual dysfunction [15]. Jasarevic *et al.* reported that exposure to BPA at low doses can affect sexual behaviors, even with no changes in sexual phenotypes or hormones [16]. Furthermore, Zhang *et al.* reported that low-dose BPA exposure could directly disrupt steroidogenesis in human cells [17]. It seems that exposure to BPA might affect human reproductive health by complicated mechanisms that encompass more than just estrogen receptor (ER) mediated pathways.

In this study, to better understand the molecular basis of the effects of BPA on human reproductive health, a genome-wide screen was performed using human foreskin fibroblast cells (hFFCs) derived from child HS patients to identify novel targets of low-dose BPA exposure. Furthermore, the effect of BPA on the global gene expression profile of hFFCs was compared with that of 17β-estradiol (E2) and 2,3,7,8-tetrachlorodibenzo-p-dioxin (TCDD), which are representative agonists of ER and aryl hydrocarbon receptor (AhR) signaling pathways, respectively.

Materials and Methods

Samples

hFFCs from child HS ($n=23$; median age 2.3 yrs) and CO ($n=11$; median age 2.3 yrs) patients undergoing surgical procedures were obtained from the National Research Institute for Child Health and Development, Japan, during 2007–2009. All subjects were of Japanese origin and written informed consent was obtained from the guardians on the behalf of the children participants involved in this study. This study was approved by the Institutional Ethics Committees of the Nagoya City University Graduate School of Medical Sciences, the National Research Institute for Child Health and Development and the National Institute for Environmental Studies.

Table 1. Summary of genes differentially expressed in response to BPA, E2 and TCDD.

	BPA		E2		TCDD	
P-value	1.0-fold	1.2-fold	1.0-fold	1.2-fold	1.0-fold	1.2-fold
0.05	154	71*	1101	814*	1150	824*
0.01	30	17	198	154	208	156
0.001	7	5	16	11	14	9

*Selected as significant differentially expressed genes and used for the network generation and pathway analysis.
doi:10.1371/journal.pone.0036711.t001

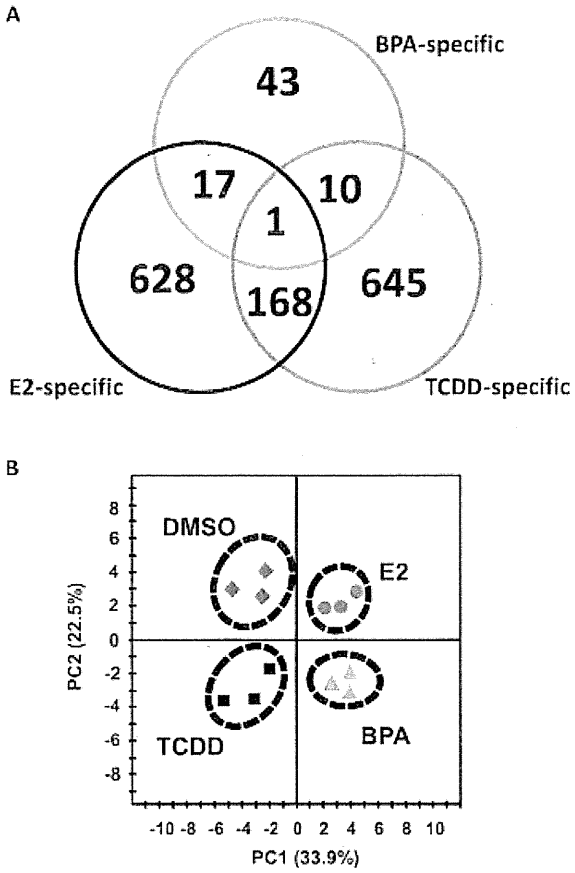

Figure 1. Genetic response of hFFCs to BPA, E2 and TCDD. (*A*) Venn-diagrams showing the number of genes that were considered significantly deregulated among the three treatment groups. (*B*) PCA scoreplot from transcript data of three hFFC cultures treated with DMSO, 10 nM BPA, 0.01 nM E2 and 1 nM TCDD.
doi:10.1371/journal.pone.0036711.g001

Chemicals

Dimethyl sulfoxide (DMSO) and E2 were obtained from Sigma Chemical Co. (St. Louis, MO, USA). BPA was obtained from Wako Industries (Osaka, Japan) and TCDD was obtained from Cambridge Isotope Laboratories (Cambridge, MA, USA). DMSO was used as the primary solvent for all chemicals, and the DMSO solutions were further diluted in cell culture media for treatments. The final concentrations of DMSO in media did not exceed 0.1% (vol/vol).

Cell culture

hFFCs were maintained in Dulbecco's Modified Eagle Medium (DMEM)/Ham's F-12 (048-29785, Wako, Osaka, Japan) containing 10% fetal bovine serum (FBS, Mediatech, Herndon, VA, USA) and grown at 37°C in a 5% CO_2 humidified incubator. For growth under steroid-free conditions, cells were seeded in phenol red-free DMEM/Ham's F-12 (045-30665, Wako) containing 5%

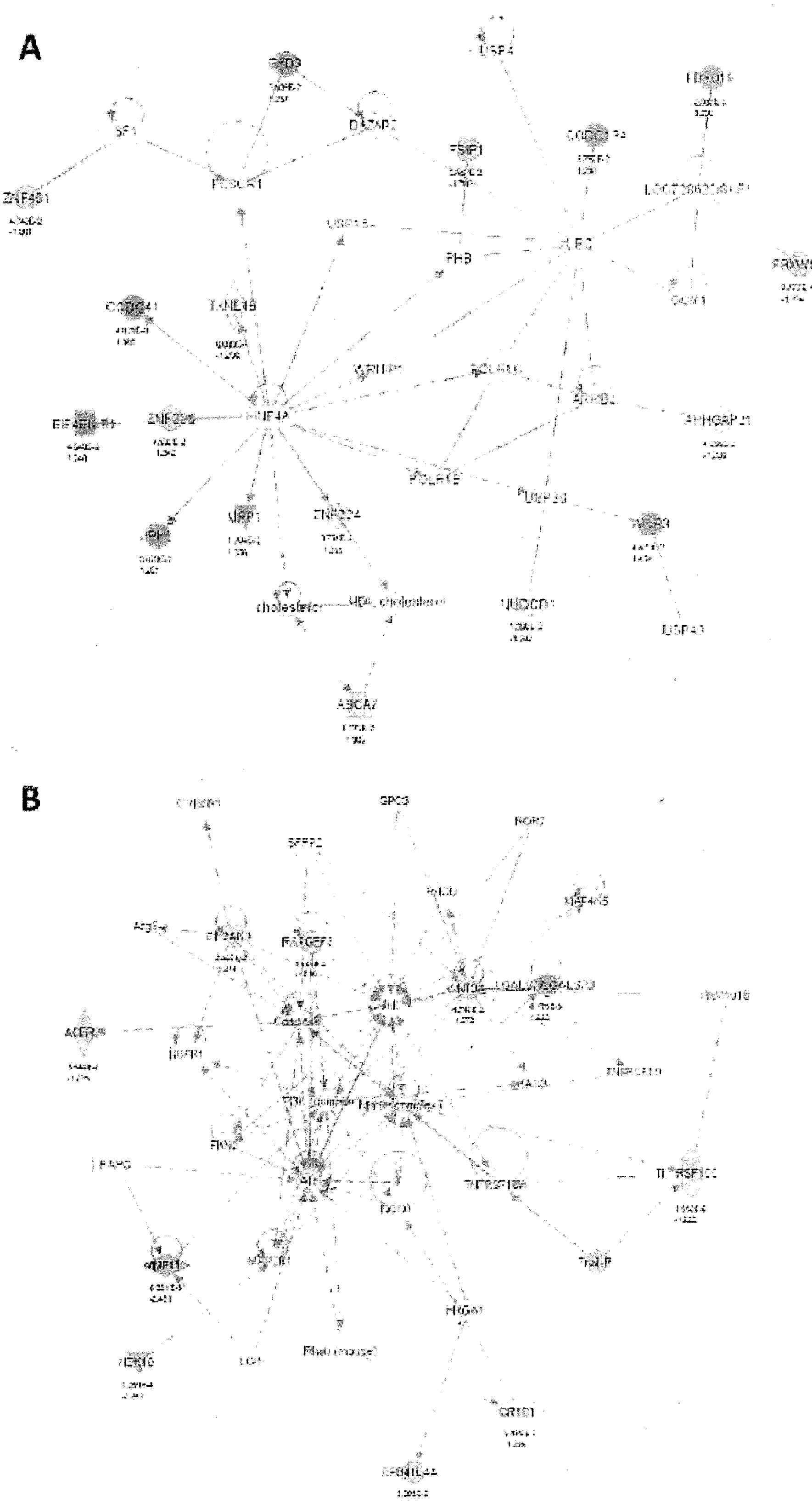
A
PHB
HNF4A
ABCA7
B

Figure 2. Network associated genes differentially expressed in response to BPA. (*A*) "Endocrine System Disorders, Gastrointestinal Disease, Genetic Disorder" network and (*B*) "Cell Death, Cellular Growth and Proliferation, Cancer" network. The images were created using the IPA platform by overlaying the differentially expressed genes in response to BPA detected by Agilent microarray analysis onto a global molecular network from the Ingenuity knowledgebase. Red indicates upregulated genes, green indicates downregulated genes, and white indicates genes that were not annotated in this array but that form part of this network. The bottom numbers indicate the fold changes induced by BPA, and the top numbers are the *P*-values between the DMSO control group and the BPA treated group. Direct relationships are exhibited with solid arrows and indirect relationships with dashed arrows.
doi:10.1371/journal.pone.0036711.g002

charcoal/dextran-treated FBS (Hyclone, Logan, UT, USA). All culture media contained 100 U/ml penicillin/streptomycin and 2 mmol/L L-glutamine (Mediatech, Herndon, VA, USA).

RNA isolation and DNA microarray analysis

Total RNA was isolated from cultured cells after treatment with chemicals for 24 h using an RNeasy Kit (Qiagen, Valencia, CA, USA) in accordance with the manufacturer's instructions. Quantification and quality assessment of the isolated RNA samples were performed and verified using an Agilent Bioanalyzer2100 (Agilent Technologies, Palo Alto, CA, USA) and a NanoDrop spectrophotometer (NanoDrop products, Wilmington, DE, USA) in accordance with the manufacturer's instructions. RNA was amplified into cRNA and labeled according to the Agilent One-Color Microarray-Based Gene Expression Analysis protocol (Agilent Technologies). Samples were then hybridized to G4851A SurePrint G3 Human GE 8×60K array slides (60,000 probes, Agilent Technologies). The slides were processed according to the manufacturer's instructions without any modification. The arrays were scanned using an Agilent Microarray Scanner (G2565BA, Agilent Technologies).

MIAME

All data are MIAME compliant, and the raw data have been deposited in the Gene Expression Omnibus (www.ncbi.nlm.nih.gov/geo, accession no. GSE35034).

Array data analysis

The scanned images were analyzed using the standard procedures described in the Agilent Feature Extraction software 9.5.3.1 (Agilent Technologies). Data analysis was performed with GeneSpring GX12.0.2 (Agilent Technologies). Signal intensities for each probe were normalized to the 75th percentile without baseline transformation. Genes that were differentially expressed following chemical treatments were identified by the unpaired Student's t test with P values cut off at 0.05 and fold change of more than 1.2 and were used for the network generation and pathway analysis.

Network generation and pathway analysis

The Ingenuity Pathways Analysis (IPA) program (Ingenuity Systems, Mountain View, CA, USA; http://www.ingenuity.com) was used to identify networks and canonical pathways of genes differentially expressed in response to BPA, E2 and TCDD. IPA software uses an extensive database of functional interactions that are drawn from peer-reviewed publications and manually maintained [18]. For the IPA analysis, the Agilent SurePrint G3 Human GE 8×60 K Array was used as a reference gene set. The generated biological networks were ranked by score, which is the likelihood of a set of genes being found in the networks owing to random chance, identified by a Fisher's exact test. The generated canonical pathways were ranked by P values, which is calculated using a Fisher's exact test by comparing the number of user-specified genes of interest that participate in a given function or pathway, relative to the total number of occurrences of these genes in all functional/pathway annotations stored in the Ingenuity

Table 2. Top five associated network functions of genes differentially expressed in response to BPA, E2 and TCDD generated by IPA.

Chemical	Top Functions	Score
BPA	Endocrine System Disorders, Gastrointestinal Disease, Genetic Disorder	41
	Cell Death, Cellular Growth and Proliferation, Cancer	21
	Cellular Growth and Proliferation, Hematological System Development and Function, Cellular Development	18
	Cellular Assembly and Organization, Cellular Function and Maintenance, Cell Cycle	13
	Dermatological Diseases and Conditions, Inflammatory Disease	3
E2	Cellular Growth and Proliferation, Skeletal and Muscular System Development and Function, Cell Cycle	41
	DNA Replication, Recombination, and Repair, Gene Expression, Cellular Assembly and Organization	41
	Cellular Assembly and Organization, Cellular Function and Maintenance, Protein Synthesis	41
	Gene Expression, Cell Cycle, Cell-To-Cell Signaling and Interaction	35
	DNA Replication, Recombination, and Repair, Nucleic Acid Metabolism, Small Molecule Biochemistry	33
TCDD	Post-Translational Modification, Genetic Disorder, Hematological Disease	49
	Cell Cycle, Cellular Assembly and Organization, DNA Replication, Recombination, and Repair	47
	Cellular Assembly and Organization, DNA Replication, Recombination, and Repair, Decreased Levels of Albumin	45
	DNA Replication, Recombination, and Repair, Energy Production, Nucleic Acid Metabolism	44
	DNA Replication, Recombination, and Repair, Cell Cycle, Cellular Assembly and Organization	37

doi:10.1371/journal.pone.0036711.t002

Table 3. Top canonical pathways for genes differentially expressed in response to BPA, E2 and TCDD identified by IPA.

Chemical	Top canonical pathway	P-Value
BPA	RAN Signaling	5.31E-02
	Endoplasmic Reticulum Stress Pathway	6.34E-02
	Leukocyte Extravasation Signaling	1.24E-01
	Retinoic acid Mediated Apoptosis Signaling	1.54E-01
	Colorectal Cancer Metastasis Signaling	1.93E-01
E2	Cell Cycle: G1/S Checkpoint Regulation	1.01E-03
	PI3K/AKT Signaling	1.52E-03
	Role of NFAT in Regulation of the Immune Response	1.83E-03
	p53 Signaling	3.46E-03
	Aryl Hydrocarbon Receptor Signaling	3.63E-03
TCDD	Cell Cycle Control of Chromosomal Replication	1.20E-09
	Role of BRCA1 in DNA Damge Response	1.72E-07
	Mismatch Repair in Eukaryotes	2.47E-05
	Hereditary Breast Cancer Signaling	9.45E-04
	Role of CHK Proteins in Cell Cycle Checkpoint Control	1.00E-02

doi:10.1371/journal.pone.0036711.t003

Pathways Knowledge Base [19]. In addition, genes significantly differentially expressed in response to BPA, E2 and TCDD was analyzed by Pathway Express (http://vortex.cs.wayne.edu/projects.htm) and mapped to Kyoto Encyclopedia of Genes and Genomes (KEGG) pathways by KegArray (http://www.kegg.jp/kegg/download/kegtools.html).

Quantitative real-time reverse-transcription polymerase chain reaction (RT-PCR)

cDNA was synthesized using a High Capacity RNA-to-cDNA Kit (Applied Biosystems, Foster City, CA, USA) according to the manufacturer's instructions. Real-time PCR was performed using TaqMan® Gene Expression Master Mix (Applied Biosystems) in accordance with the manufacturer's instructions. TaqMan® Gene Expression Assays (Applied Biosystems) used in this study were: Hs02341150_m1 for POMZP3, Hs01094348_m1 for WDR3, Hs00171829_m1 for metallopeptidase 11 (MMP11; see gene names in Table S1), and Hs00266705 g1 for glyceraldehyde-3-phosphate dehydrogenase (GAPDH). The primers (Forward: 5'-TGTTGGGGGATAAGGACAAA-3'; and Reverse: 5'-GCAGGCTGTACAGGAACCAT-3') and probe (5'-TAAACT-CACCTCTGTGGTTGGAACAAT-3') for NEK10 were designed and synthesized by Hokkaido System Science (Sapporo, Hokkaido, Japan). The amplification reaction was performed in an ABI PRISM 7000 Sequence Detector (Applied Biosystems) under the following cycling conditions: 95°C for 15 min, followed by 40 cycles of 95°C for 15 s and 60°C for 60 s. The gene expression levels were calculated based on the threshold cycle using Sequence Detection System Software (Applied Biosystems). Gene expression was normalized to that of GAPDH and set to 100 for the control DMSO-treated cells.

Statistical and multivariate analysis

Quantitative data were expressed as the mean ± SEM. A nonparametric test, the Mann-Whitney U test, was applied to test for statistical significance. Values of $P<0.05$ were considered to indicate statistical significance. Unsupervised principal component analysis (PCA) was run in SIMCA-P+ (Version 12.0, Umetrics, Umeå, Sweden) to obtain a general overview of the variance of genes differentially expressed in response to BPA, E2 and TCDD.

Results

Gene expression profiles of hFFCs in response to BPA, E2 and TCDD

The gene expression profiles in hFFCs treated with DMSO control or 10 nM BPA, 0.01 nM E2 or 1 nM TCDD were determined by Agilent microarray analysis using three biological replicates. Then, differentially expressed genes in response to BPA, E2 and TCDD compared with DMSO control were identified by the unpaired Student's t test with P values cut off at 0.05 and fold change of more than 1.2 using GeneSpring GX software. Seventy-one genes (42 downregulated and 29 upregulated), 814 genes (371 downregulated and 443 upregulated), and 824 genes (344 downregulated and 480 upregulated) were identified to be significantly differentially expressed in response to BPA, E2, and TCDD, respectively. No nuclear receptor was found to be significantly differentially expressed in response to BPA, while estrogen-related receptor-α (ESRRA), retinoic acid receptor-α (RARA) and RAR-related orphan receptor-α (RORA) and RARA were found to be significantly differentially expressed in response to E2 and TCDD, respectively. The summary of differentially expressed genes along with their P values and fold changes is provided in Table 1.

Differences in the response of hFFCs to BPA, E2 and TCDD

Comparison of the gene expression profiles of hFFCs in response to BPA, E2 and TCDD is provided in Figure 1. BPA-specific responses were found in 43 significantly differentially expressed genes, compared with responses to E2 and TCDD (Figure 1A). Seventeen and 10 differentially expressed genes were found to be common in response to BPA with E2 or TCDD, respectively. A full list of these genes is summarized in Table S1.

Furthermore, to compare the expression patterns of hFFCs in response to BPA with that of E2 or TCDD, PCA analysis was performed on the data of significantly differentially expressed genes in response to BPA. PCA is a standard technique of pattern recognition and multivariate data analysis. Of interest, the cells treated with DMSO, BPA, E2 and TCDD were clearly distinguished from each other by the PCA score plots (Figure 1B). According to the first component (PC1), which represents 33.9% of the total variance, a very clear discrimination between cells treated with BPA or E2 and those treated with DMSO or TCDD was observed. However, according to the second component (PC2), which represents 22.5% of the total variance, cells treated with BPA or TCDD were clearly distinguished from those treated with DMSO or E2. It should be noted that differences in the PCA were identified using an unsupervised analysis, without any prior information on the samples. Since all cells were cultured under identical conditions, the observed discriminations demonstrate that the effect of BPA is similar to that of E2 according to PC1 but is similar to that of TCDD according to PC2.

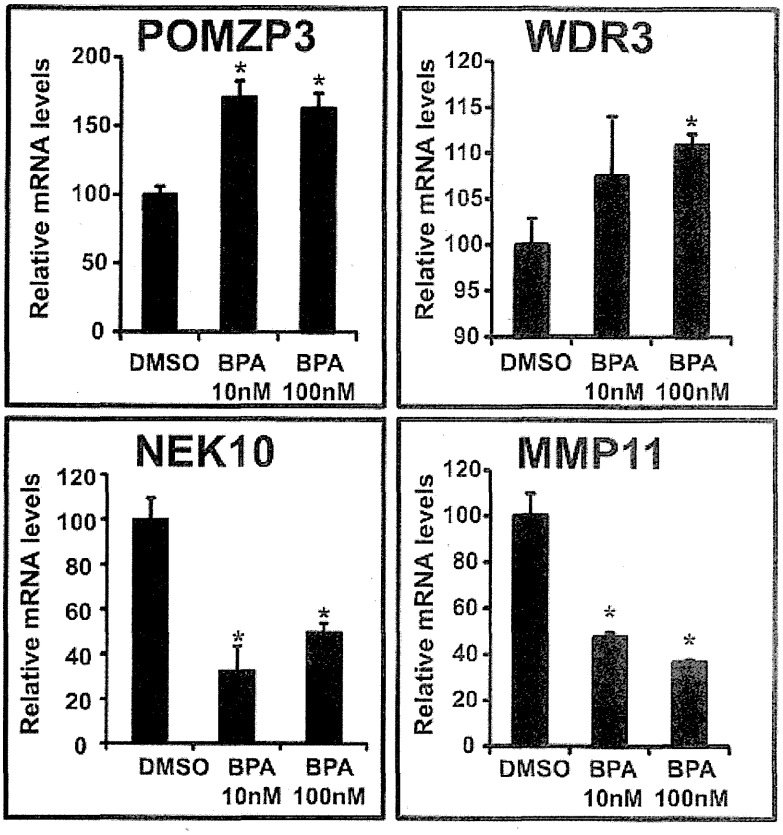

Figure 3. Validation of POMZP1, WDR3, NEK10 and MMP11 expression. Cells were treated with BPA at 10 nM and 100 nM for 24 h, and then the expression of POMZP1, WDR3, NEK10 and MMP11 was examined by real-time PCR. *$P<0.05$ vs. DMSO control cells.
doi:10.1371/journal.pone.0036711.g003

Network generation and pathway analysis of genes differentially expressed in response to BPA, E2 and TCDD

To investigate possible biological interactions of differently regulated genes, datasets derived from microarray analysis representing genes with altered expression profiles were imported into the IPA platform. Network analysis of the biological functions of the top five IPA-generated networks is summarized in Table 2 and is shown in Figure 2 and Figure S1,S2,S3.The two most highly populated biological networks entitled "Endocrine System Disorders, Gastrointestinal Disease, Genetic Disorder" (Score = 41) and "Cell Death, Cellular Growth and Proliferation, Cancer" (Score = 21) were identified with genes differentially expressed in response to BPA (Figure 2). The networks consisted of genes that encoded enzymes (ACER2, PLSCR1, POLR1C, TXNL4B and UBC), peptidases (MMP11, UCHL5, USP4, USP36 and USP43), proteins that regulate transcription (ABCA7, CRTC1, HNF4A, LOC728622/SKP1, PHB, SF1 and SLC25A6) and translation (EIF4ENIF1 and TNFRSF10C), and others (ARHGAP21, ARRB2, CCDC41, CCDC134, EIF2AK3, EPB41L4A, DAZAP2, EPB41L3, EXD3, FBXO18, FBXW12, FSIP1, JRKL, LGALS7/LGALS7B, NEK10, NUDCD1, RAPGEF3, SERPINA1, WDR3, WNT3A, ZNF222, ZNF224 and ZNF461). The most highly populated biological networks were identified with genes differentially expressed in response to E2 and TCDD and were entitled "Cellular Growth and Proliferation, Skeletal and Muscular System Development and Function, Cell Cycle" (Score = 41) and "Post-Translational Modification, Genetic Disorder, Hematological Disease" (Score = 49), respectively. Furthermore, top canonical pathways associated with genes significantly differentially expressed in response to BPA, E2 and TCDD were summarized in Table 3. The pathway most affected by BPA is "RAN Signaling" with only borderline significance ($P = 0.0531$). The pathways most affected by E2 and TCDD are "Cell Cycle: G1/S Checkpoint Regulation" and "Cell Cycle Control of Chromosomal Replication", respectively ($P = 1.01\times10^{-3}$ and 1.20×10^{-9}, respectively).

In addition, a list of top KEGG pathways affected by BPA, E2 and TCDD identified by Pathway Express was summarized in Table S2. By inputting the list of genes significantly differentially expressed in response to BPA, E2 and TCDD into Pathway Express, 12 KEGG pathways, but without statistical significance, were found to be affected by BPA, while 27 and 9 KEGG pathways were found to be significantly affected by E2 and TCDD, respectively. As an example, "Pathways in cancer" of KEGG mapped with genes significantly differentially expressed in response to BPA, E2 and TCDD using KegArray was illustrated in Figure S4.

Validation by real-time PCR

To validate the microarray data and to identify potential biomarkers for BPA toxicity in hFFCs derived from HS patients, the expression of the most up- or down-regulated genes (POMZP3, 1.46-fold; WDR3, 1.45-fold; NEK10, 0.44-fold;

A

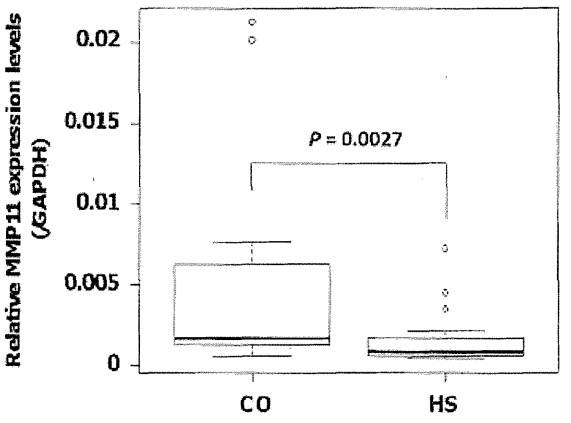

B

	n	Relative MMP11 expression levels (/GAPDH) (mean ± SEM)
CO	11	0.0058 ± 0.0022
HS	23	0.0015 ± 0.00033

Figure 4. Reduced levels of MMP11 expression in hFFCs derived from child HS patients. Significantly lower MMP11 expression was observed in hFFCs derived from the HS ($n = 23$) group compared with the CO ($n = 11$) group by TaqMan real-time PCR. (*A*) Boxplot and (*B*) summary of the quantitative data comparing MMP11 expression levels in HS and CO groups.
doi:10.1371/journal.pone.0036711.g004

MMP11, 0.41-fold) in response to BPA was validated by real-time PCR. As the results show in Figure 3, the PCR data showed good concordance with the microarray data in terms of the expression direction (up- or down-regulation). A significant increase in the mRNA levels of POMZP3 and WDR3 and a significant decrease in the mRNA levels of NEK10 and MMP11 were observed following BPA treatments at high and/or low concentrations (10 nM and 100 nM, respectively).

Comparison of MMP11 expression levels in hFFCs derived from child HS and CO patients

To further investigate the potential role of MMP11 in the development of HS, we examined the expression levels of MMP11 in hFFCs derived from child HS and CO patients ($n = 23$ and 11, respectively). As shown Figure 4, the mean MMP11 expression level, normalized to GAPDH, in the HS group was 0.0015 and in the CO group, 0.0058. Significantly lower MMP11 expression levels were observed in the HS group compared with the CO group (0.25-fold, $P = 0.0027$).

Discussion

To better understand the molecular basis of the effects of BPA on human reproductive health, target genes of low-dose BPA exposure were identified in hFFCs derived from child HS patients using DNA microarray analysis. Human foreskin tissues obtained from patients with HS have been used as *in vitro* models to define the etiology of HS [20–22]. However, these investigations have not delineated the relative contribution of environmental factors. To our knowledge, our study is the first report to use hFFCs to investigate the potential effects of BPA on the development of HS. The concentration of BPA used to treat the cells in our microarray analysis was 10 nM, which is below the dose of 50 μg/kg/day (approximately 200 nM for *in vitro* cell or organ culture studies) usually considered as safe for humans [7]. Moreover, this dose is in the concentration range of 1–19.4 nM that is commonly detected in human tissues and fluids [4].

In this study, we compared the gene expression profiles of hFFCs in response to BPA, E2 and TCDD. Using PCA, we found that the effect of BPA is similar to that of E2 according to PC1 but is similar to that of TCDD according to PC2. Forty-three genes were found to be affected exclusively by BPA, underscoring the concept that the effects observed are ER and AhR-independent (Figure 1). In our previous study, we examined the estrogenic activity of BPA in estrogen receptor 1 (ESR1)-positive BG1Luc4E2 human ovarian cancer cells and found that BPA increased the ESR1-induced luciferase activity in a dose-dependent manner with a lowest observed effect at 100 nM [23]. Although differences exist between cell lines, it is possible that the underlying mechanisms of the endocrine-disrupting effects of BPA at doses lower than the reference limits might involve pathways other than estrogen signaling. Indeed, differences in transcript profiles in response to BPA and E2 have been previously described in ESR1-positive human cells [24]. Furthermore, amore recent study reported that BPA might lead to severe malformation during vertebrate embryogenesis, while no effects were seen with exposure to the E2 or ER-antagonist ICI 182,780 [25].

It is not unexpected that the largest biological network identified by IPA analysis with genes differentially expressed in response to BPA was entitled "Endocrine System Disorders, Gastrointestinal Disease, Genetic Disorder" (Table 2 and Figure 2A). It should be noted that this network contains three genes (ZNF222, ZNF224 and ZNF461) that belong to the zinc finger protein (ZFP) family. ZFPs are among the most abundant proteins in eukaryotic genomes and play various roles in the regulation of transcription [26]. The biological function of ZNF222 and ZNF461 remains to be investigated, but ZNF224 participates in key cellular processes, such as regulation of cell growth [27]. Previous reports have revealed that ZNF224 might play a critical role in bladder carcinogenesis by regulating the apoptosis of bladder cancer cells [28]. None of these three ZNFs have been previously associated with the development of HS. However, two other zinc finger box genes, ZEB1 and ZEB2, have been associated with HS [20,29]. Our data indicate that ZFP-mediated transcriptional activity might be required for the effect of BPA on human reproduction. It is known that zinc finger structures are as diverse as their functions [26]. Therefore, it is likely that further investigations into the function of ZFPs in transcriptional regulation will provide novel insights to explain the association we found between ZFP expression and low-dose BPA exposure regarding the pathogenesis of HS.

The expression of four of the significantly differentially expressed genes identified in the microarray analysis was verified by real-time PCR analysis. Of particular interest, MMP11 (0.47-fold and 0.37-fold at 10 nM and 100 nM, respectively), which is involved in the "Cell Death, Cellular Growth and Proliferation, Cancer" network, was shown to be down-regulated (Figures 2B and 3). The matrix metalloproteinases (MMPs) are zinc-dependent endopeptidases that are involved in the breakdown of extracellular matrix (ECM) in normal physiological processes, such as embryonic development, reproduction, and tissue remodeling, as well as in disease processes, such as arthritis and metastasis [30,31]. It is well known that MMP11 is overexpressed in several human cancers, including breast, cervix, colon, ovary, prostate,